# APPENDIX F

SBM Accidental Release Modelling in Support of the Equinor Bay du Nord Development Project (RPS 2018)

# SBM Accidental Release Modelling in Support of the Equinor Bay du Nord Development Project

Prepared for: Equinor Canada Ltd.

**Project Number:**
**2018-P-022447**

**Date Submitted:**
**10/19/2018**

**Version:**
Final Report

**Project Manager**
Matthew Horn, Ph.D.

RPS
55 Village Square Dr.
South Kingstown, RI USA
02879-8248

| Release | File Name | Date Submitted | Notes |
|---|---|---|---|
| Final | Equinor– RPS Technical Report_20181019.docx | 10/19/2018 | Final RPS report for review by Equinor |
| Draft | Equinor– RPS Technical Report_20180828.docx | 08/28/2018 | RPS Draft report for review by Equinor |
| Draft | Equinor– RPS Technical Report_20180824.docx | 08/24/2018 | RPS Draft report following senior technical review |
| Draft | Equinor– RPS Technical Report_20180822.docx | 08/22/2018 | RPS Internal Draft version of report following team review |
| Draft | Equinor– RPS Technical Report_20180808.docx | 08/08/2018 | RPS Internal Draft version of report |

# List of Contributors

Matthew Horn, PhD – Project Lead and Senior Scientist

matt.horn@rpsgroup.com

Daniel Torre—Environmental Chemist, drilling discharges modeller and report preparation

Nathan Vinhateiro—Senior Oceanographer, report review

Steven Tadros—Scientist, report preparation

Tayebeh TajalliBakhshs—Oceanographer, Metocean data preparation

Mahmud Monim – Oceanographer, Metocean data preparation

Jenna Ducharme – GIS Specialist, figure generation

Matthew Frediani –GIS Analyst, figure generation

Alicia Morandi – Environmental Analyst, report preparation

Deborah French McCay – Senior Scientist, report review

Cheryl Morse – Programmer/Developer

Timothy Giguere – Programmer/Developer

# Executive Summary

The accidental release of synthetic based mud was modelled to support an Environmental Impact Statement (EIS) for the Bay du Nord Development Project. The Project Area includes portions of the easternmost edge the Flemish Pass, as well as the northwestern portion of the Flemish Cap. Modelling was performed at representative sites that were located approximately 450-500 km east of the St. John's, Newfoundland, with drilling anticipated in waters that range in depth from <350 m to >1200 m. Hypothetical deterministic simulations were performed at two locations, Site 1 and Site 2 to represent (i) a surface release of 60 $m^3$ of SBM associated with the accidental discharge of a full mud tank from the drilling platform , (ii) a subsurface release of 275 $m^3$ of SBM associated with the accidental discharge from a failure at a flex joint near the seabed, and (iii) a subsurface full riser release of 275 $m^3$ of SBM associated with the disconnection of the riser at the Blow Out Preventer (BOP). Site 1 is representative of drilling in the Core BdN Development area at water depths of approximately 1100-1200 m. This site is also within a designated Vulnerable Marine Area as it is Fishery Closure Area. Site 2 is representative of drilling in shallower waters in the larger Project Area, should future development activities occur. Each of these simulations was performed for two different current regimes (twelve total simulations) to evaluate how ocean current variability in the region may affect the patterns of SBM dispersion. The water depths are approximately 1,134 m for Site 1 and 500 m for Site 2.

Discharge simulations were completed using RPS's MUDMAP modelling system. The MUDMAP model is used to predict the transport of solids releases in the marine environment and the resulting seabed deposition. The model inputs include information regarding the discharge characteristics (release location, rate of discharge, etc.), the properties of the sediment (particle sizes, density), as well as environmental characteristics (bathymetry and ocean currents), to predict the transport of solids through the water column. The model output consists of the movement and shape of the discharge plume, the concentrations of insoluble discharge components in the water column, and the accumulation of discharged solids on the seabed. The model predicts the transport of solid particles from the time of discharge or release to initial settling on the seabed. MUDMAP does not account for resuspension and transport of previously discharged solids; therefore, it provides a conservative estimate of the potential seafloor depositions.

Bathymetry was characterized using databases provided by NOAA National Geophysical Data Center and GEBCO. Currents for the North Atlantic region were acquired from the three-dimensional HYCOM (HYbrid Coordinate Ocean Model) circulation model. For this study, daily current data were obtained, and trends were analyzed for the period of January 2006 through December 2012 for the North Atlantic region. As with any hydrodynamic model, there is the potential that local currents may deviate from

predictions based upon grid resolution and small-scale variability in ocean circulation dynamics. However, the data used is sufficient for this type of modelling.

Three deterministic simulations were conducted for two release locations, for two different current regimes, totaling twelve simulations. Runs were initialized with different release parameters including depth of release, current regimes, release rates, release durations, and SBM settling velocities to best characterize the range of potential seabed depositions and water column concentrations resulting from an accidental release of SBM.

At both drilling locations, measurable thicknesses (0.1 mm) were predicted to result from accidental releases of SBM in the project site and were expected to remain within 1.5 km of the spill location. Surface releases of SBM would be expected to result in seabed deposition extending farthest from the spill location, due to intensified currents at the surface, slower settling time, and a greater depth over which to settle. The depth of each release site had the greatest potential to increase the extent of deposition but also generally reduced the predicted total thicknesses of the deposit. In the simulation results, the extent of deposition from surface releases was intensified by prevailing currents during winter conditions. Subsurface releases occurring from a BOP disconnect near the seafloor would be expected to result in thicker deposition over a smaller area than other scenarios, due to the faster settling time of particles released from a wide, low velocity flow incident.

The variations within predicted results between simulations were due to three main factors including: 1) release height relative to the seabed, 2) settling velocity associated with low versus high velocity releases, and 3) current patterns. Releases resulting from accidental mud tank spillage and BOP disconnect occur at a lower flow rate, and therefore would have faster settling times and thicker deposition within an area that is close to the spill site. Specifically, areal extent affected by surface releases are the most different across site due to difference in depth. Flex joint failure releases typically resulted in increased flow rate, making particles much smaller and therefore decreasing settling rates, which allowed for particles to travel further before being deposited on the seafloor.

The releases modelled in this study may be considered representative of other potential releases in the project area. The water depths at Site 1 and Site 2 (1,134 and 500 m, respectively) are similar in depth to other potential drilling locations in the area.

The hypothetical accidental releases modelled in this study are not intended to predict a specific future event, but rather are to be used as a tool in environmental assessments to predict potential area of interaction. The results presented in this document demonstrate that there are a range of potential trajectories that could result if a release of synthetic based drilling mud were to occur. The specific trajectories vary for each release based upon the nature of the release, the environmental conditions,

and the properties of the fluids. While each accidental release is unique and therefore uncertainties exist, the results of this modelling study suggest that if SBM were to be released in the project Area, there is the potential for seabed deposition > 0.1mm to extend 1.5 km from the spill site. In addition, there is the potential for water column concentrations to exceed 10,000 mg/L within 10 m of the spill locations, however these concentrations are only reached momentarily during the initialization of the release and are not expected to persist.

**Document Summary**

This report includes an introduction describing the region, the modelling approach, the methodology, and finally the results of the study. The model results are summarized in figures and tables in the main body of this document, describing the potential for SBM contamination within the water column and on the seabed. This document is broken down into several sections. Section 1 includes an introduction to the modelling study. Section 2 includes a description of project area, modelling approach using the MUDMAP model, scenarios, and uncertainty. Section 3 contains a description of the model input data. Section 4 summarizes the seabed deposition and water column concentration model results. Section 5 summarizes conclusions and discussion points. Section 6 contains the references cited. Additional information may be found in supporting Appendix A, which provides a detailed description of the MUDMAP model, fates processes, and algorithms used.

# Table of Contents

# List of Figures

# List of Tables

# List of Acronyms and Abbreviations

BOP: Blow out preventer

EIS: Environmental Impact Statements

Site 1: Eastern Flemish Pass hypothetical release location 1 (1,134 m depth)

Site 2: Eastern Flemish Pass hypothetical release location 2 (500 m depth)

FJF: Flex Joint Failure

GEBCO: The General Bathymetric Chart of the Oceans operated by the International Hydrographic Organization (IHO) and Intergovernmental Oceanographic Commission (IOC) of UNESCO.

HYCOM: The U.S. Navy HYbrid Coordinate Ocean Model used for currents

MICOM: Miami Isopycnic-Coordinate Ocean Model

NCODA: U.S. Navy Coupled Ocean Data Assimilation

NOAA: U.S. National Oceanic and Atmospheric Administration

NRC: U.S. National Research Council

NRDA: The U.S. Natural Resource Damage Assessment

SBM: Synthetic based mud

SwRI. The Southwest Regional Institute

# 1 Introduction

RPS (previously Applied Science Associates, Inc.) conducted drilling discharge modelling in support of an Environmental Impact Statement (EIS) for Equinor Canada Ltd. Bay du Nord Development Project. The EIS Project Area is located approximately 450 km east of the Newfoundland coast. Water depths in the Project Area range from <350 m to >1200 m. Major currents, including the Labrador Current and the Gulf Stream, influence the circulation and biological productivity in this region.

Simulations of accidental synthetic based mud (SBM) releases were completed using RPS's MUDMAP modelling system (Spaulding et al., 1994). MUDMAP predicts the transport of solids released in the marine environment and the resulting seabed deposition. The model requires inputs describing: (i) the physical and chemical characteristics of the discharged effluent, (ii) the discharge timing and release location, and (iii) information describing the receiving waters (bathymetry, density structure, ocean currents). Model output includes estimates of environmental loadings to the seabed (deposition) and water column (increased turbidity) from discharges associated with offshore drilling. A technical description of the MUDMAP model is included in Appendix A.

# 2 Background and Scenarios

## 2.1 Project Area

Newfoundland is comprised of a series of islands off the east coast of Canada, and along with Labrador forms the easternmost Canadian province. The relatively shallow waters of the continental shelf extend eastward into the northwest Atlantic Ocean up to 500 km off the Newfoundland coast. The Equinor Project Area (49-49.5 °N, 45-46.5 °W) contains portions of the Grand Banks, Flemish Pass, and Flemish Cap east of Newfoundland (Table 2-1 and Figure 2-1). Bathymetry in the area ranges from less than 100 m over the Grand Bank to greater than 1,200 m deep in the Labrador Basin.

**Table 2-1. Hypothetical release locations within the Bay du Nord Project Area.**

| Site Name | Latitude | Longitude | Water Depth (m) |
|---|---|---|---|
| Site 1 | 47.96°N | 46.21°W | 1,134 |
| Site 2 | 47.89°N | 47.04°W | 500 |

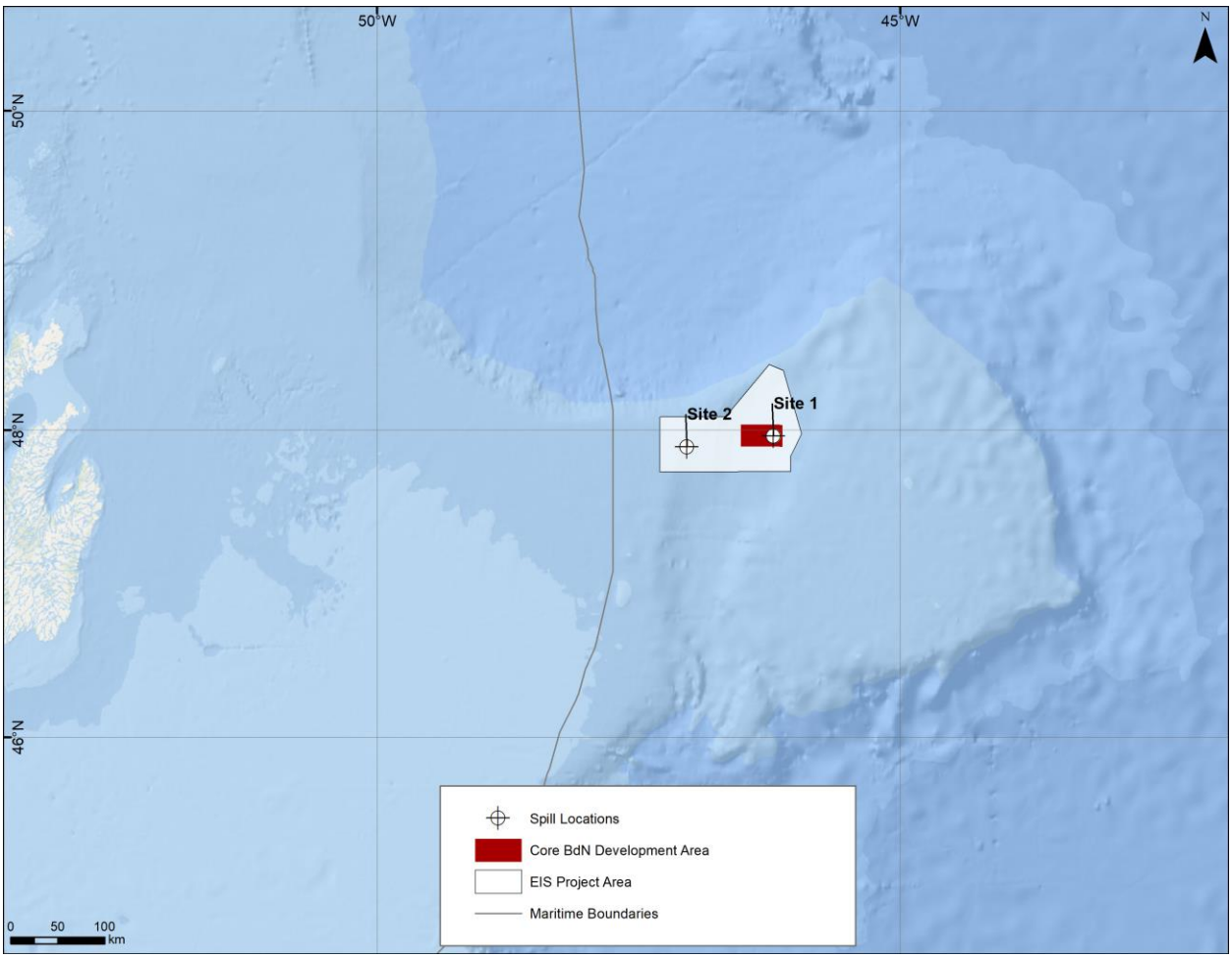


**Figure 2-1. Map of the Project Area, including the two hypothetical release locations: Site 1 and Site 2.**

## 2.2 Modelling Approach

Information provided by Equinor Canada Ltd. indicates that SBMs will be used during development drilling. Site 1 is representative of drilling in the Core BdN Development area at water depths of approximately 1100-1200 m. This site is also within a designated Vulnerable Marine Area as it is NAFO Fishery Closure Area (Northwest Flemish Cap [10]). Site 2 is representative of drilling in shallower waters in the larger Project Area, should future development activities occur. The criteria for simulations to be modelled were identified by Equinor Canada Ltd. For both sites, deterministic simulations were performed to represent (i) a surface release of 60 $m^3$ of SBM associated with the accidental discharge of a full mud tank from the drilling platform, (ii) a subsurface release of 275 $m^3$ of SBM associated with the accidental discharge from a failure at a flex joint near the seabed (20 m above seafloor), and (iii) a subsurface full riser release of 275 $m^3$ of SBM associated with the disconnection of the riser at the Blow

Out Preventer (BOP), at a depth of approximately 20 meters above the seafloor. Each of these simulations was performed for two representative release locations under two different current regimes (twelve total simulations) to evaluate how ocean current variability in the region may affect the patterns of SBM dispersion.

Information provided by Equinor indicates that a 1,350 kg/m$^3$ Paradril-IA LV SBM system will be used during drilling operations. Settling velocity distributions presented in a Southwest Research Institute (SwRI) study from 2007 were used in MUDMAP to represent characteristics of the SBM system for each of the individual modelling simulations. SwRI (2007) presents settling velocities for a range of SBM's under different flow regimes, ranging from release velocities of 20 cm/s for wide orifice diameters to 278 cm/s release velocities for narrow orifices. In general, faster release rates result in smaller particle sizes and therefore slower settling velocities. Based off specific gravity, Mud D referenced in SwRI's experiments was the closest representation to the SBM identified by Equinor and was used as a representative analog mud for these modelling efforts.

Drilling operations are planned to take place year round. In order to evaluate the influence of variability in ocean currents on the deposition pattern in the Project Area, MUDMAP simulations were developed for two current regimes (representative of fall and winter) at each drilling site (Table 2-2). Fall and winter were chosen to capture a range of met ocean conditions which would result in different predicted magnitudes and extents potentially affected. Specific simulation periods were selected based on a review of recent literature and an analysis of ocean circulation models within the drilling project region (discussed further in Section 3.1). October 15$^{th}$, 2010 and January 15$^{th}$, 2011 were chosen as representative release dates for Fall and Winter, respectively, because they were identified in the aforementioned analysis to best capture the differences in seasonality in the region. Each simulation covered a minimum period of approximately 6 hours to allow ample time for dispersion and settling.

**Table 2-2. Site and release information used for each scenario.**

| Site Name | Release Description | Season | Discharge Volume ($m^2$) | Duration of Release (hour) | Discharge Flow Type | Depth of Release (m) |
|---|---|---|---|---|---|---|
| Site 1 | Surface Tank | Winter | 60 | 0.5 | Wide, low speed jet | 5 m below surface |
| | | Fall | | | | |
| Site 2 | Surface Tank | Winter | | | | |
| | | Fall | | | | |
| Site 1 | Riser Flex Joint | Winter | 275 | 3 | Narrow, high speed jet | 20 m above seafloor |
| | | Fall | | | | |
| Site 2 | Riser Flex Joint | Winter | | | | |
| | | Fall | | | | |
| Site 1 | BOP Disconnect | Winter | 275 | 1 | Wide, low speed jet | 20 m above seafloor |
| | | Fall | | | | |
| Site 2 | BOP Disconnect | Winter | | | | |
| | | Fall | | | | |

### 2.2.1 Modelling Tool - MUDMAP

Drilling discharge simulations were completed using RPS's MUDMAP modelling system (Spaulding et al., 1994). MUDMAP is a numerical model developed by RPS to predict the near- and far-field transport, dispersion, and bottom deposition of drilling mud and cuttings. In MUDMAP, the equations governing conservation of mass, momentum, buoyancy, and solid particle flux are formulated using integral plume theory and then solved using a Runge Kutta numerical integration technique. The model includes three stages: convective descent/ascent, dynamic collapse, and far field dispersion. It allows the transport and dispersion of the release to be modelled through all stages of its movement. The initial dilution and vertical spreading of the release is predicted in the convective descent/ascent process. The far field process predicts the transport and dispersion of the release caused by the ambient current and turbulence fields. In the dynamic collapse process, the release impacts the surface or bottom, or becomes trapped by vertical density gradients in the water column.

MUDMAP is widely used to simulate settling and dispersion of drilling mud and cuttings for offshore environmental impact assessments and follows the same theoretical framework as several other common cuttings models (IOGP 2016). The equations and solutions in MUDMAP are based on thirty years of research and the model is regularly updated as new scientific research is presented. The system has been applied for discharge operations in both coastal and offshore environments and has shown excellent agreement with other industry accepted models such as the Offshore Operators Committee Mud and Produced Water Discharge Model (e.g., Spaulding et al., 1994). Examples of the model validation are provided in Burns et al. (1999), King and McAllister (1997, 1998), and Tetra Tech (2002). Limitations of the MUDMAP model are similar to those that exist for most other cuttings dispersion

models (IOGP 2016), including that it does not account for certain complex process such as aggregation (or degradation) of cuttings as they settle, flocculation, or post-depositional consolidation of cuttings over time. MUDMAP does not account for the resuspension and transport of previously discharged solids; therefore, it provides a conservative estimate of the potential seafloor depositions.

The model output consists of the movement and shape of the discharge plume, the concentrations of insoluble (i.e., cuttings and mud) discharge components in the water column, and the accumulation of discharged solids on the seabed. The model predicts the transport of solid particles from the time of discharge or release to initial settling on the seabed. With simplifying assumptions, concentrations of hydrocarbons or other pollutants adhered to cuttings can be derived from the seabed loading (Nedwed, 2004). The algorithms for the far field and passive diffusion stage are based on a particle based random walk model. More details about MUDMAP are included in Appendix A.

### 2.2.2 Thresholds of Concern

#### 2.2.2.1 Sedimentation Effects and Thresholds

Although sediment deposition is a natural process, rate of sedimentation varies based on the oceanographic characteristics of the area. Deep sea habitats, like those in the current study, are generally characterized by low-energy currents and slow sediment accumulation rates of 1 – 100 mm per thousand years (Gage and Tyler, 1991; Glover and Smith, 2003). Benthic organisms associated with these environments are generally adapted to tolerate a range of conditions and sedimentation rates. Rapid increases in sedimentation associated with mud and cuttings discharges can have direct and indirect effects on benthic infauna communities in deep sea habitats. Direct effects can include smothering, toxicity exposure, and physical abrasion. Indirect effects include habitat alterations and changes to community assemblages (DOER, 2005). The severity of sedimentation effects on organisms depends on factors including burial depth, burial rate, burial time, species-specific tolerances, the grain size of the deposited sediments, and seasonal timing (Kjeilen-Eilertsen et al. 2004). For example, higher mortality can occur in the summer than in the winter (Smit et al. 2008). Higher mortality has been shown to occur at higher temperatures in mesocosm and lab studies of mussel and gastropod burial, possibly due to greater oxygen demand at higher temperatures (Chandrasekara and Frid 1998; Hutchison et al. 2016). Taxonomic groups react differently and have varying levels of tolerance for sedimentation, with sessile and attached organisms having the lowest tolerance and highest mortality rate during sedimentation events (DOER 2005; Gates and Jones 2012).

Previous research conducted on sedimentation and recovery of benthic infauna in Newfoundland, Canada, observed increased abundance and biomass in some polychaete species and declines in others

in the area around the drill site. Reduced abundance extended approximately 1 - 2 km from the drill site for some species (Paine et al., 2014). This aligns with findings from an extensive literature review that documented biological effects (such as changes in benthic community structure) at distances of 200 – 2,000 m from platforms using water-based drilling fluids (Ellis et al. 2012). The range of effects from synthetic-based drilling fluids was found to be somewhat smaller, detecting biological effects from 50 – 1,000 m from the drill site (Ellis et al. 2012).

Specific sedimentation thresholds tested and reported by Smit et al. (2008) indicate that epibenthic, sessile, filter-feeding species cannot survive sediment burial depths over 10 mm. Meanwhile, infauna taxa that are adapted to habitat covered in sediment may escape from burial under 100 mm of sediment or more (Kjeilen-Eilertsen et al. 2004). In a mesocosm and field study, Trannum et al. (2011) observed that 24 mm of water-based drill cuttings lowered oxygen availability and reduced abundance for macrofauna in the sediment. Overall, Smit et al. (2008) estimated that mortality of 5% of benthic organisms (including mollusks, polychaetes, and crustaceans) would occur at burial depths of 6.3 mm (3.1 – 10.6 mm) and mortality of 50% would occur at burial depths of 54 mm (37 – 79 mm).

Benthic invertebrates are broadly considered to be unaffected by nontoxic sediment burial depths less than 6.5 mm, based on tolerances to burial, oxygen depletion and change in sediment grain size (Wood, 2018; Kjeilen-Eilertsen et al. 2004; Smit et al. 2006; 2008). However, some more sensitive species are considered more susceptible to shallower burial depths (1.5 mm), and thus 1.5 mm is suggested as a more conservative predicted no effect threshold.

Studies on the recovery of benthic infaunal communities post-sedimentation present varying results. The ability of a benthic community to recover after sediment deposition depends on larval settlement, the rate of bioturbation, and sediment mixing by currents (Smit et al. 2008; Trannum et al. 2011). Because many benthic species have drifting pelagic larvae, resettlement can occur within months post-disturbance. Trannum et al. (2011) observed reestablishment of species-rich communities within six months of sedimentation and noted that the most successful colonizers were species in the Spionidae family of polychaete worms. In studies from the North Sea, recolonization of cuttings piles from the edges of the pile occurs in 1 – 5 years (Kjeilen-Eilertsen et al. 2004). Areas with the thickest deposition will likely rely on larval transport and resettlement for recolonization, as survival of buried organisms is unlikely. In areas with lower levels of deposition, reestablishment by surviving organisms that burrow or sift through sediment to feed is possible, as they mix mud and cuttings with native sediments and slowly return habitats to pre-drilling conditions (Smit et al. 2008; Gates and Jones 2012).

#### 2.2.2.2 Turbidity and TSS Effects and Thresholds

Smit et al. (2006, 2008) described an increase in the concentration of total suspended solids (TSS) and water column turbidity due to the discharge of drilling cuttings and fluids, which could potentially affect pelagic organisms. Particulates in drilling muds come from bentonite clay and barite, which are toxicologically inert, but can be suspended in the water column. Suspended clay particles of less than 0.01 mm diameter settle very slowly and can potentially persist in the water column for weeks or months (Smit et al. 2008).

Increased turbidity decreases the light availability for phytoplankton in the water column (IOGP, 2016). Phytoplankton were negatively affected at concentrations of 10 mg/L bentonite clay or 1,000 mg/L barite, but these concentrations are unlikely to occur in a discharge plume greater than 25 m down-current (IOGP, 2016). In general, drilling fluid and cuttings solids rapidly disperse, dilute, and settle out of the water column, which reduces the risk of adverse effects on water column organisms because exposure to elevated turbidity or TSS is intermittent and brief (IOGP, 2016).

Benthic suspension feeders (e.g., molluscs) are sensitive to mud and cuttings discharges because they are sessile organisms that cannot escape discharge plumes, and fine suspended particles interfere with feeding and growth (DOER 2005; Smit et al. 2008). Filter-feeding zooplankton and algae were also more sensitive, likely due to greater exposure in the water column from drifting with the currents and therefore with portions of the discharge plume that encounter surface currents. Benthic crustaceans and siphon-feeding molluscs were relatively insensitive to suspended particulates, likely because they have evolved to inhabit the benthic boundary layer comprising mobile sediments and water that is naturally highly turbid (Smit et al. 2008). However, the quality of data available to evaluate TSS thresholds is poor, with few lab studies on bentonite or barite suspended clays.

Synthetic non-aqueous base fluids are not considered toxic to phytoplankton, zooplankton, and other water column marine organisms (IOGP, 2016). Certain chemicals within synthetic base fluids (primary emulsifier and fluid loss agent) elicited sublethal exposure responses in biomarkers of juvenile pink snapper fish, which suggests that chronic exposure from chemicals leaching out of cuttings piles may have some effect on fish over several days (Bakhtyar and Gagnon, 2012). However, a transient exposure to drilling fluids as they pass through the water column is unlikely to be toxic to mobile pelagic organisms.

# 3 Model Input Data

## 3.1 Circulation and Currents

The Labrador Current dominates the large-scale ocean circulation in the Newfoundland region originating in the Arctic Ocean and flowing south along the coasts of Labrador and Newfoundland (Figure 3-1). This southerly current intensifies as waters funnel through the offshore branch, which follows the Flemish Pass between the Grand Banks and Flemish Cap. To a lesser extent, a portion of the Labrador Current flows through an inshore branch, which follows the Avalon Channel between Newfoundland and the Grand Banks. Over parts of the Grand Banks, currents can be generally weak and flow southward (Statoil, 2016). Maximum current speeds in the upper 200 m of the water column range from 0.3 – 2.0 m/s (C-NLOPB, 2014). The strong southerly current dominates the yearly average flow and winds may only account for approximately 10% of current variability in this region (Petrie and Isenor, 1985). South of the Flemish Pass, the Labrador Current mixes with the North Atlantic current. The boundary where these two currents converge produces extremely energetic and variable frontal systems and eddies on smaller scales, on the order of kilometers (Volkov, 2005). Due to these eddies, local transport may advect parcels of water in nearly any direction. Satellite and drifter studies of current dynamics demonstrate this complexity; however, drifting parcels generally move to the south and east (Han and Tang, 1999; Petrie and Anderson, 1983; Richardson, 1983) where they intersect with the North Atlantic current.

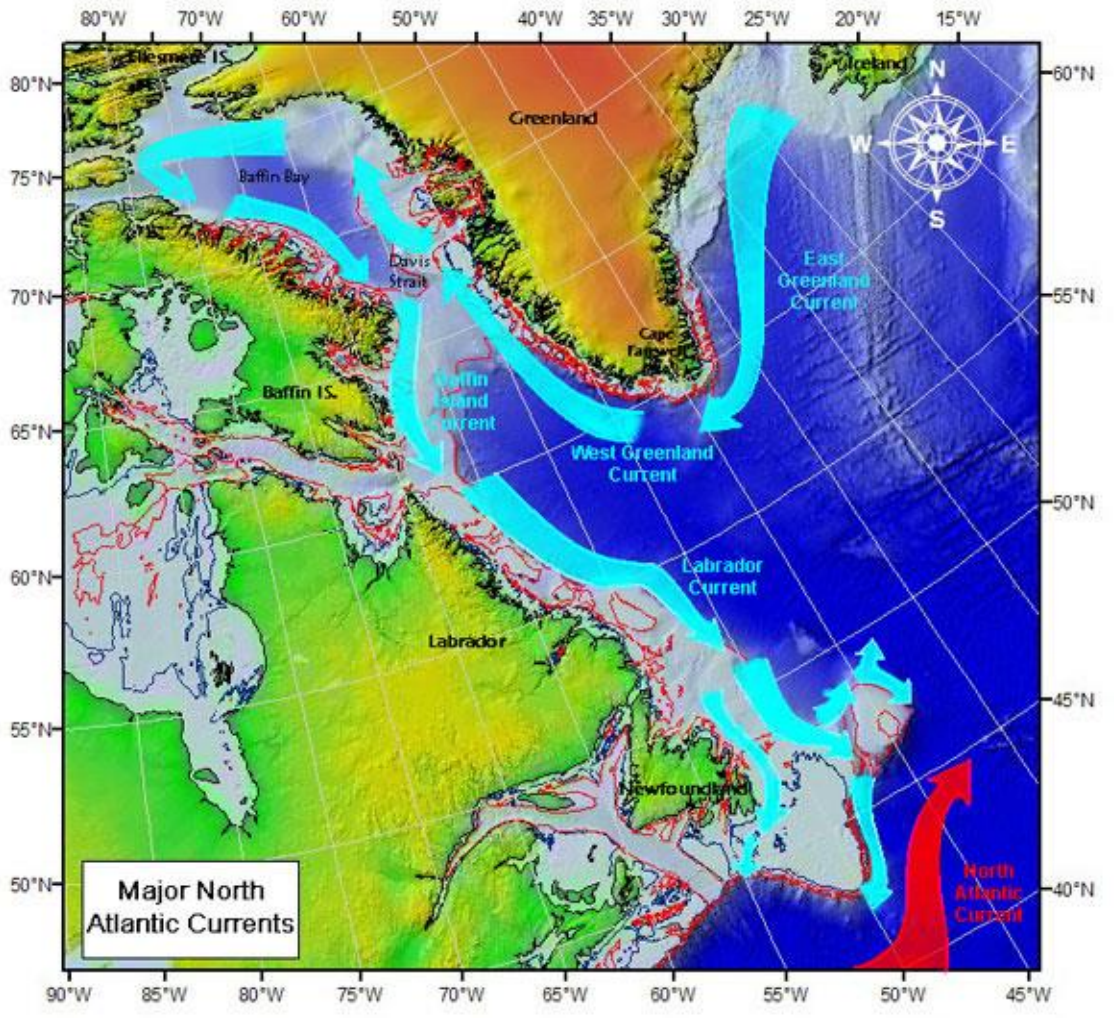


**Figure 3-1. Large scale ocean currents in the Newfoundland region (USCG 2009).**

Currents for the North Atlantic region were acquired from the HYCOM (HYbrid Coordinate Ocean Model) circulation model. HYCOM is a primitive-equation ocean general circulation model that evolved from the Miami Isopycnic-Coordinate Ocean Model (MICOM) (Halliwell, 2002; Halliwell et al., 1998, 2000; Bleck, 2002). MICOM has become one of the premier ocean circulation models, having been subjected to validation studies (Chassignet et al., 1996; Roberts et al., 1996; Marsh et al., 1996) and used in numerous ocean climate studies (New and Bleck, 1995; New et al., 1995; Hu, 1996; Halliwell, 1997, 1998; Bleck, 1998). The HYCOM global ocean system is a 3D dynamic model and uses Mercator projections between 78° S and 47° N and a bipolar patch for regions north of 47° N to avoid computational problems associated with the convergence of the meridians at the pole. The 1/12° equatorial resolution provides gridded ocean data with an average spacing of ~7-8 km between each

point. Data is assimilated through the Navy Coupled Ocean Data Assimilation (NCODA) system (Cummings, 2005). The NCODA system employs a Multi-Variate Optimal Interpolation scheme, which uses model forecasts as a first guess and then refines estimates from available satellite and in-situ temperature and salinity data that are applied through the water column using a downward projection of surface information (Cooper and Haines, 1996). Bathymetry is derived from the U.S. Naval Research Laboratory BDB2 dataset. Surface forcing is derived from the Navy Operational Global Atmospheric Prediction System, which includes wind stress, wind speed, heat flux (using bulk formula), and precipitation. Surface forcing of HYCOM is derived from 1-hourly CFSR wind data with a horizontal resolution of 0.3125° and induced wind stress, wind speed, heat flux, and precipitation with bathymetry derived from the GEBCO dataset (HYCOM, 2016).

The HYCOM surface current pattern for the area of interest for the period of 2006-2012 (Figure 3-2) illustrates that the sites are very close to the location where Labrador Current divides into two branches near Flemish Cap. The HYCOM monthly current roses at Site 1 does not have any clear seasonality in terms of speed or directions (Figure 3-3). However, the current roses at Site 2 illustrate that a larger portion of the current directions ranges from east to north during April-June period, while for the rest of the year currents are primarily directed to the south and east (Figure 3-4). Monthly surface current speeds (cm/s) derived from the HYCOM model at both sites are moderate, with monthly average current speed around 20-35 cm/s and $95^{th}$ percentile current speed 40-70 cm/s (Figure 3-5). Maximum current speeds are predicted during September at Site 2 (153 cm/s) and August in Site 1 (130 cm/s). Vertical current profiles and current roses for Site 1 and Site 2 are presented in Figure 3-6 and Figure 3-7, respectively. The figures compare the distribution of flow at various depths from the HYCOM grid cell that contains the drilling sites. In addition, horizontal current vector (cm/s) time series at five different depths for each location are used to portray current speed and direction at different water levels (Figure 3-8 and Figure 3-9). Both the vertical profiles and the current vectors illustrate that the current speed decreases as the depth increases. Surface currents head to the east (varying from north to south) at both drilling sites. The currents at mid layer and bottom layer are heading mainly to the south-southwest at Site 1 and oscillate between north and south direction at Site 2.

All figures display current data in the oceanographic convention, indicating the direction in which currents are flowing towards.

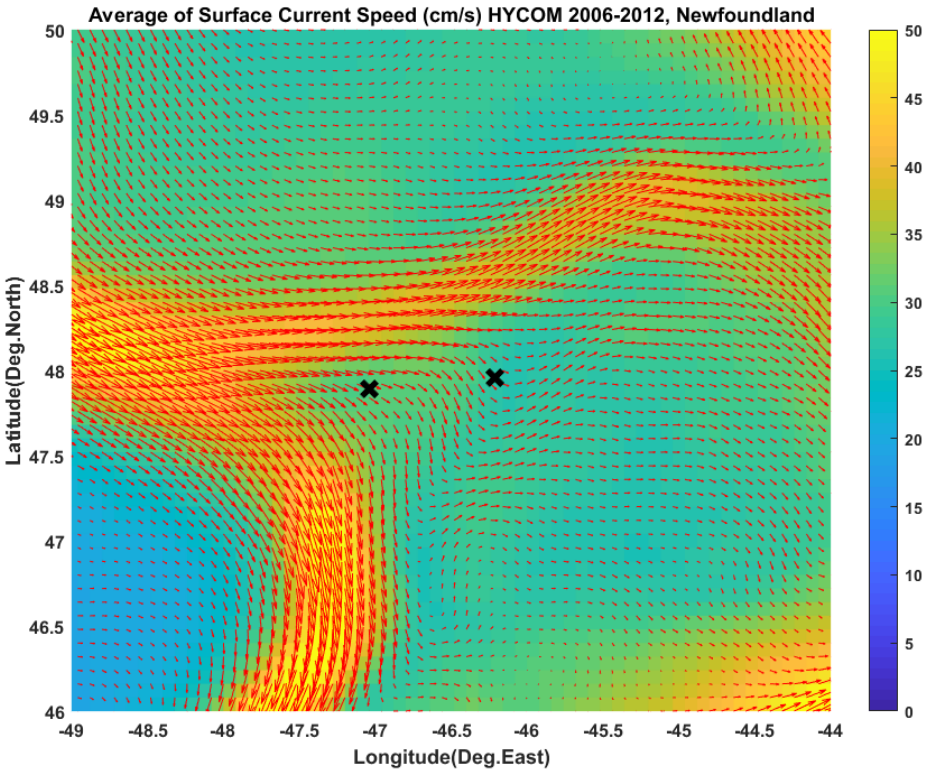


**Figure 3-2. Averaged surface current speed (cm/s) in color, and direction presented as red vectors offshore Newfoundland from HYCOM (2006 – 2012). Black X's represent the representative drilling sites.**

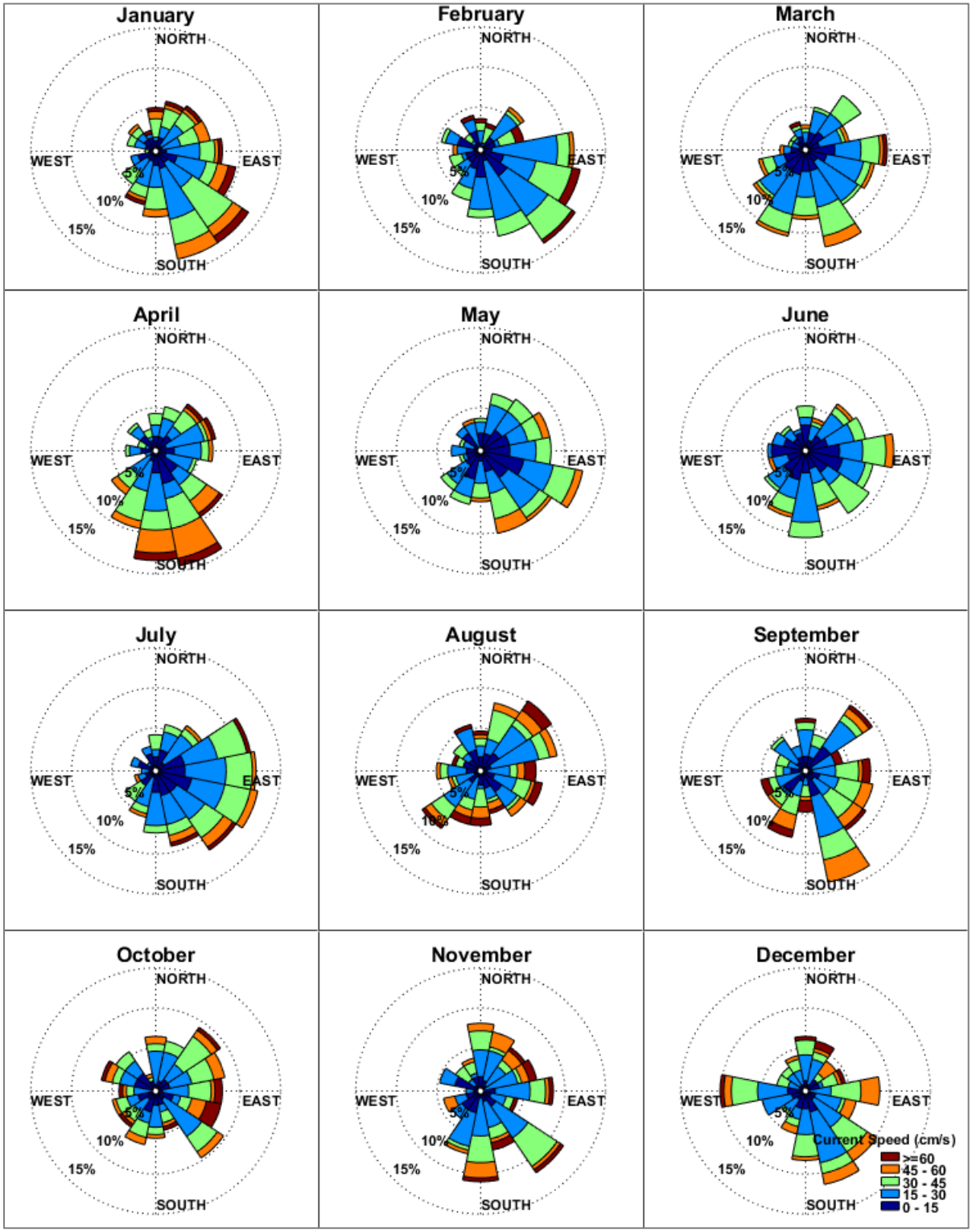


**Figure 3-3. Current roses illustrating the distribution of HYCOM surface currents (speed and direction) by month at Site 1 (model period from 2006-2012); using oceanographic convention (direction currents are flowing to).**

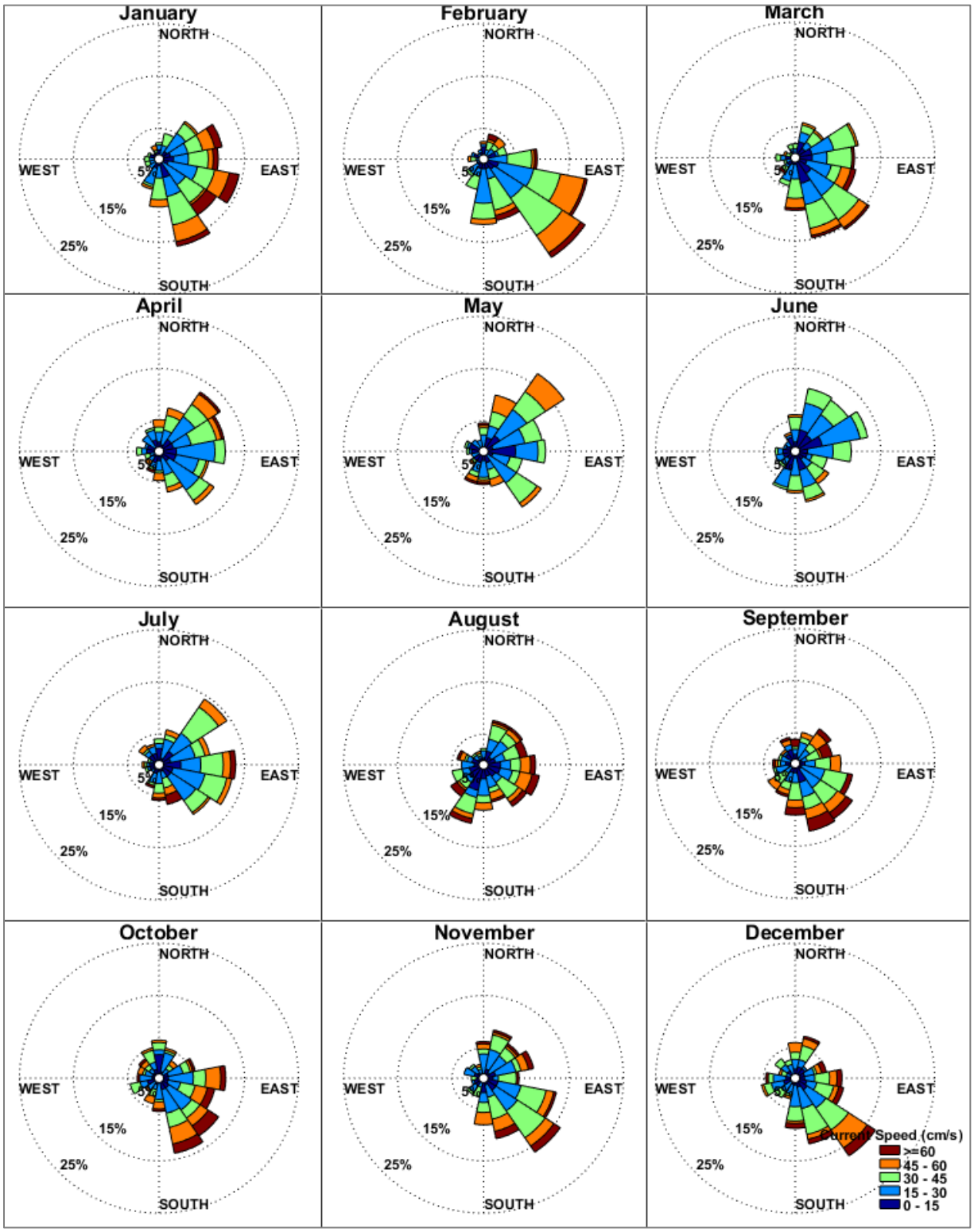


**Figure 3-4. Current roses illustrating the distribution of HYCOM surface currents (speed and direction) by month at Site 2 (model period from 2006-2012); using oceanographic convention (direction currents are flowing to).**

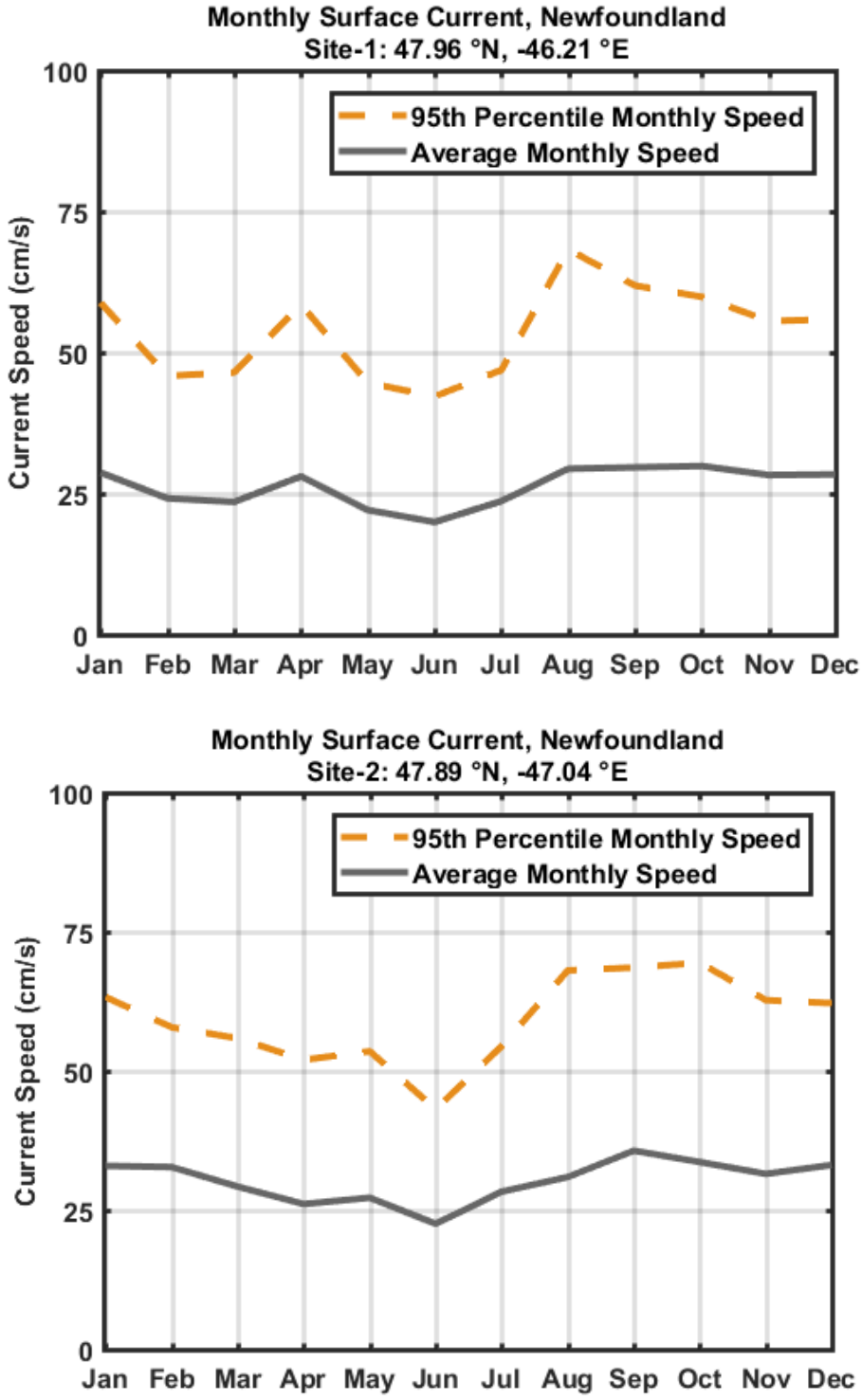


**Figure 3-5. Monthly average (grey solid) and 95$^{th}$ percentile (orange dashed) HYCOM surface current speed (cm/s) statistics near Site 1 (top) and Site2 (bottom).**

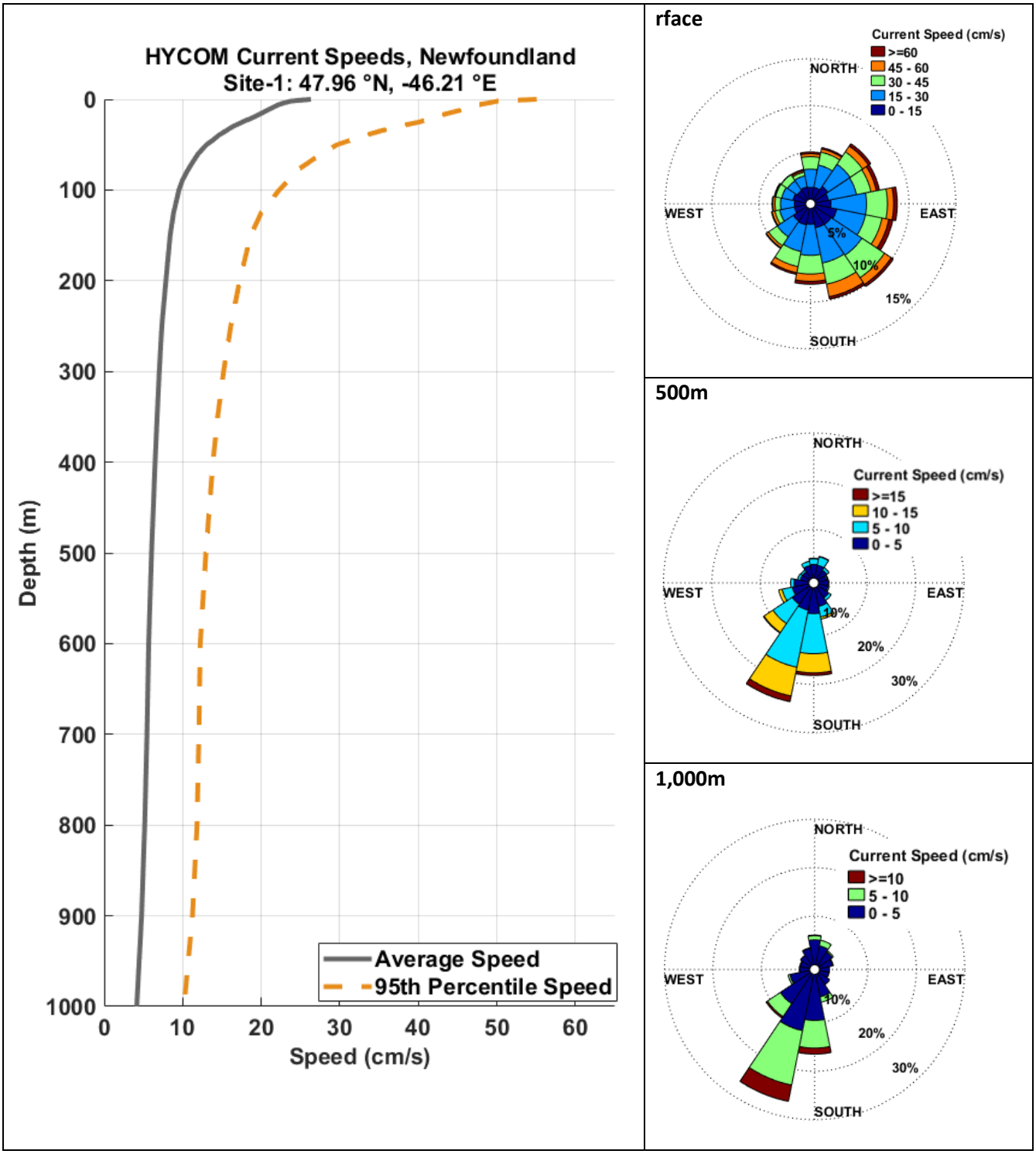


**Figure 3-6. Vertical profiles of variation in horizontal current speed (cm/s) by depth (m) (left) and current roses at multiple depths presented in oceanographic convention (direction currents are flowing to) (right) at Site 1; derived from HYCOM model currents between 2006 and 2012.**

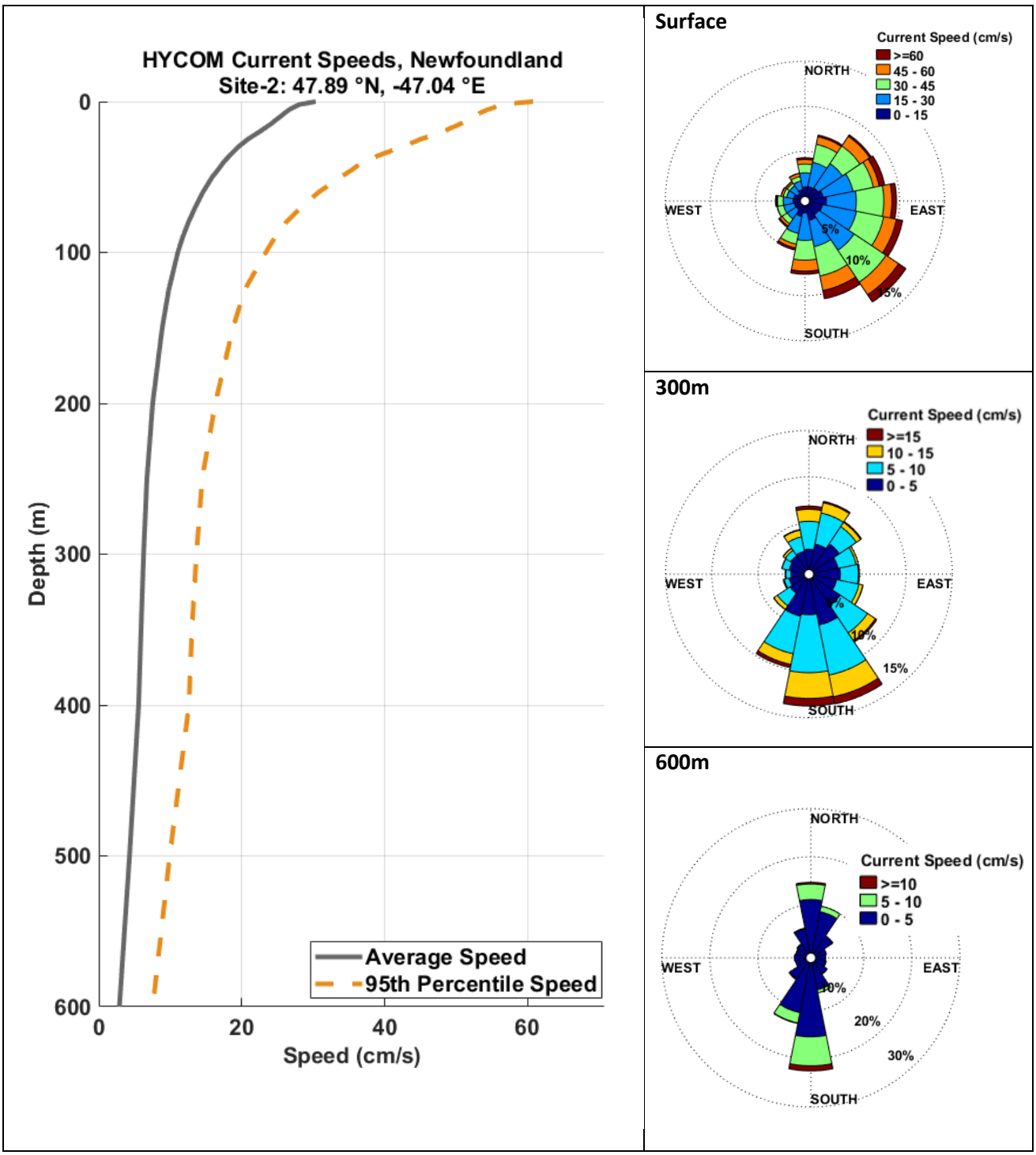


**Figure 3-7. Vertical profiles of variation in horizontal current speed (cm/s) by depth (m) (left) and current roses at multiple depths presented in oceanographic convention (direction currents are flowing to) (right) at Site 2; derived from HYCOM model currents between 2006 and 2012.**

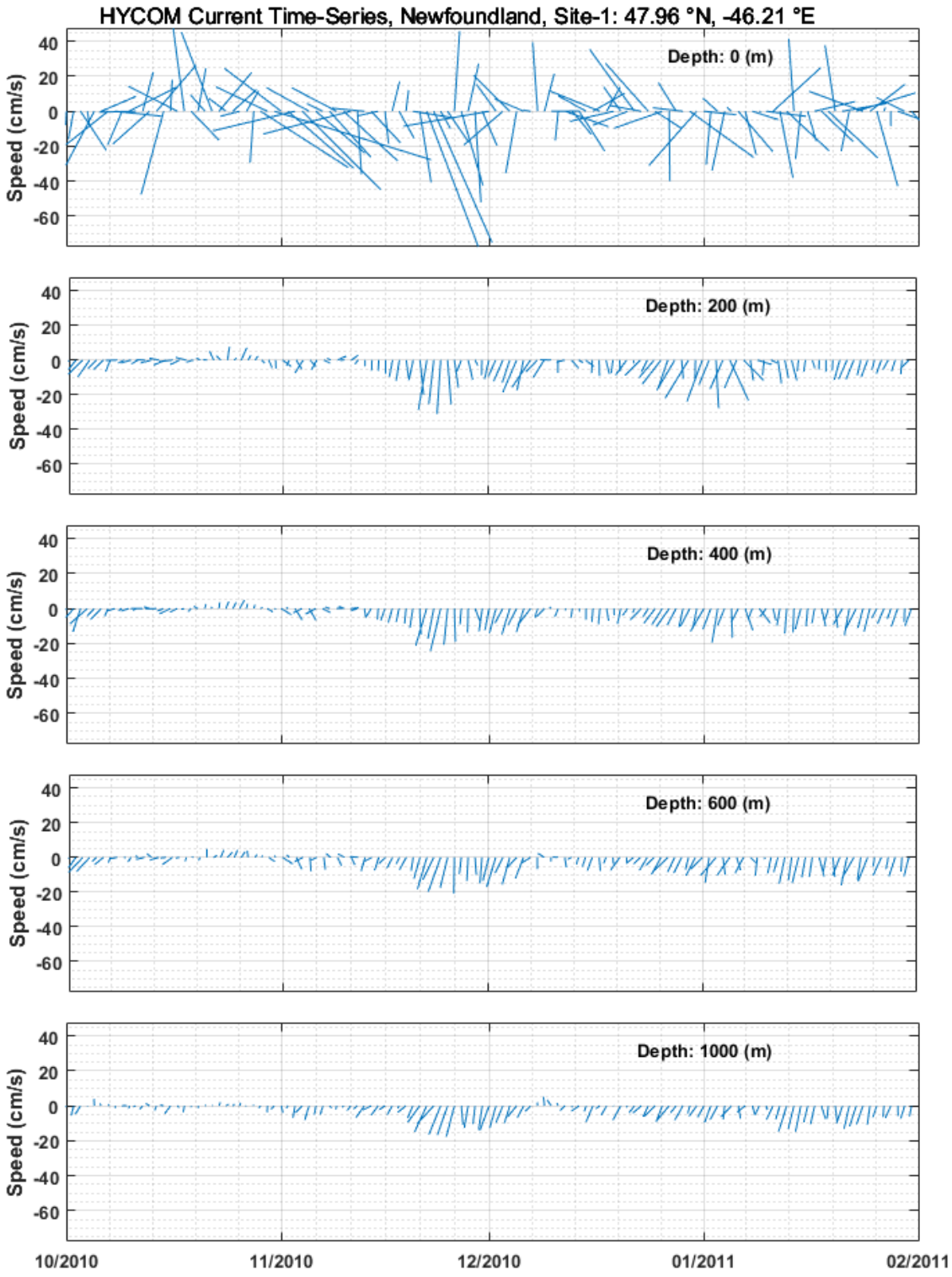


**Figure 3-8. Time series of HYCOM current speeds (cm/s) with depth (m) at Site 1. Note that the highlighted depths in this figure differ from those presented for Site 2 (Figure 3-9).**

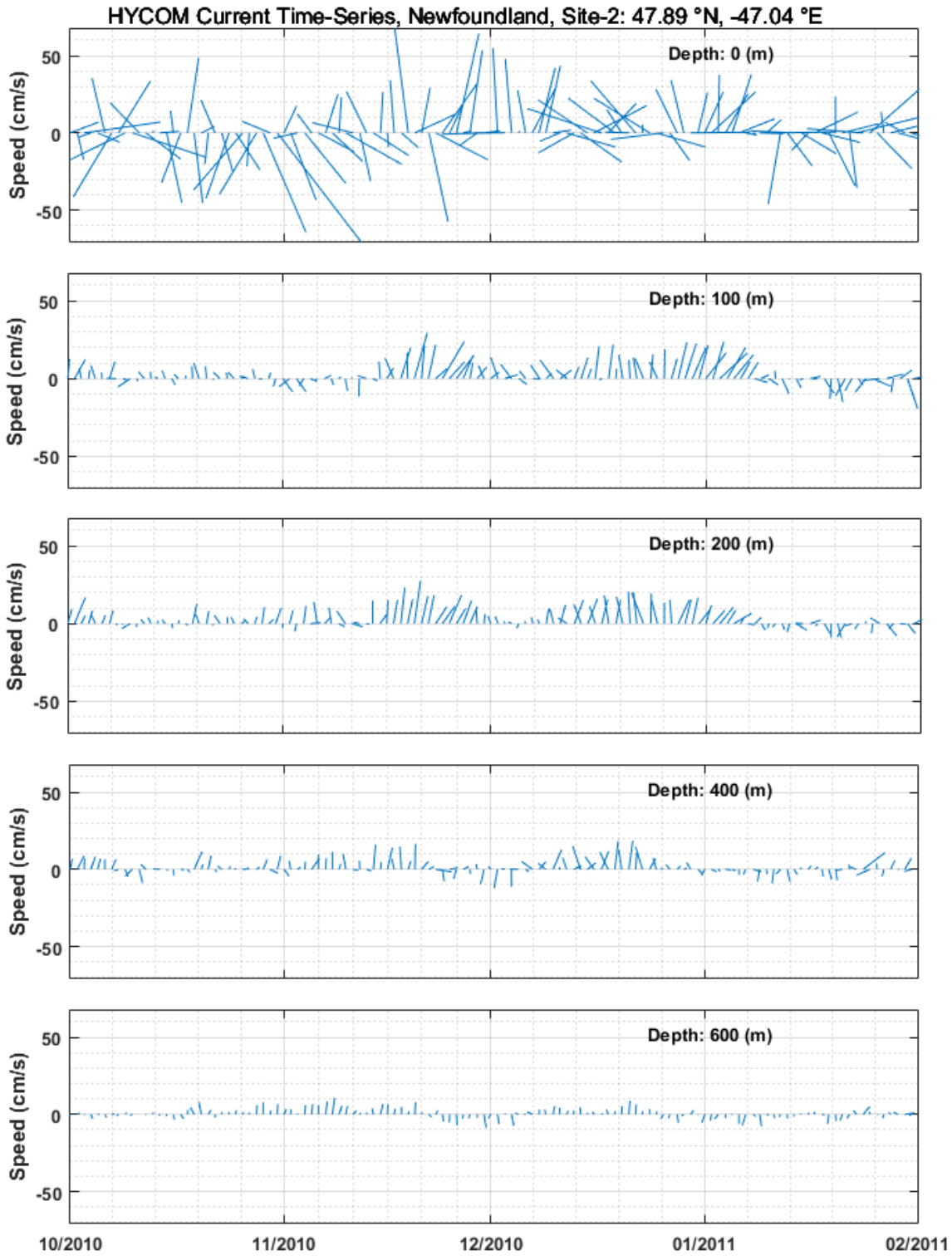


**Figure 3-9. Time series of HYCOM current speeds (cm/s) with depth (m) at Site 2. Note that the highlighted depths in this figure differ from those presented for Site 1 (Figure 3-8).**

## 3.2 Accidental SBM Releases

MUDMAP was used to simulate accidental releases of synthetic based drilling fluids at both Site 1 and Site 2. For both sites, three deterministic simulations were performed for two current regimes (12 total simulations), representing (i) a surface release of 60 $m^3$ of SBM associated with the accidental discharge of a full mud tank from the drilling platform, (ii) a subsurface release of 275 $m^3$ of SBM associated with the accidental discharge from a failure at a flex joint near the seabed (20 m above), and (iii) a subsurface full riser release of 275 $m^3$ of SBM associated with the disconnection of the riser at the BOP, which is located 20 m above the seafloor (Table 2-2). The specification of accidental release volumes and the use of a 1,350 kg/$m^3$ Paradril-IA LV SBM was provided by Equinor.

## 3.3 Discharged Solids Characteristics

To assess the fate of drilling discharges in the marine environment it is critical to characterize the components of the released materials. The composition of the drilling mud applied will depend on the characteristics of the formation being drilled and this composition determines the density and weight of the discharged fluid, its toxicity, and the settling velocities of the material released into the water column.

Settling velocities to be used in MUDMAP simulations were approximated from SwRI (2007) experimental data (Figure 3-10). The study conducted by SwRI included fall velocity tests of several SBM products under different jet velocities, which ultimately resulted in different particle size distributions and thus settling velocities. Mud D referenced in SWRI (2007), was chosen as an analog mud due to its similarity in bulk density (1,400 kg/$m^3$) to the Paradril-IA LV SBM. Settling velocities resulting from low speed and high speed jet releases of Mud D were used in these simulations to more realistically characterize the respective releases (Table 3-1 and Table 3-2).

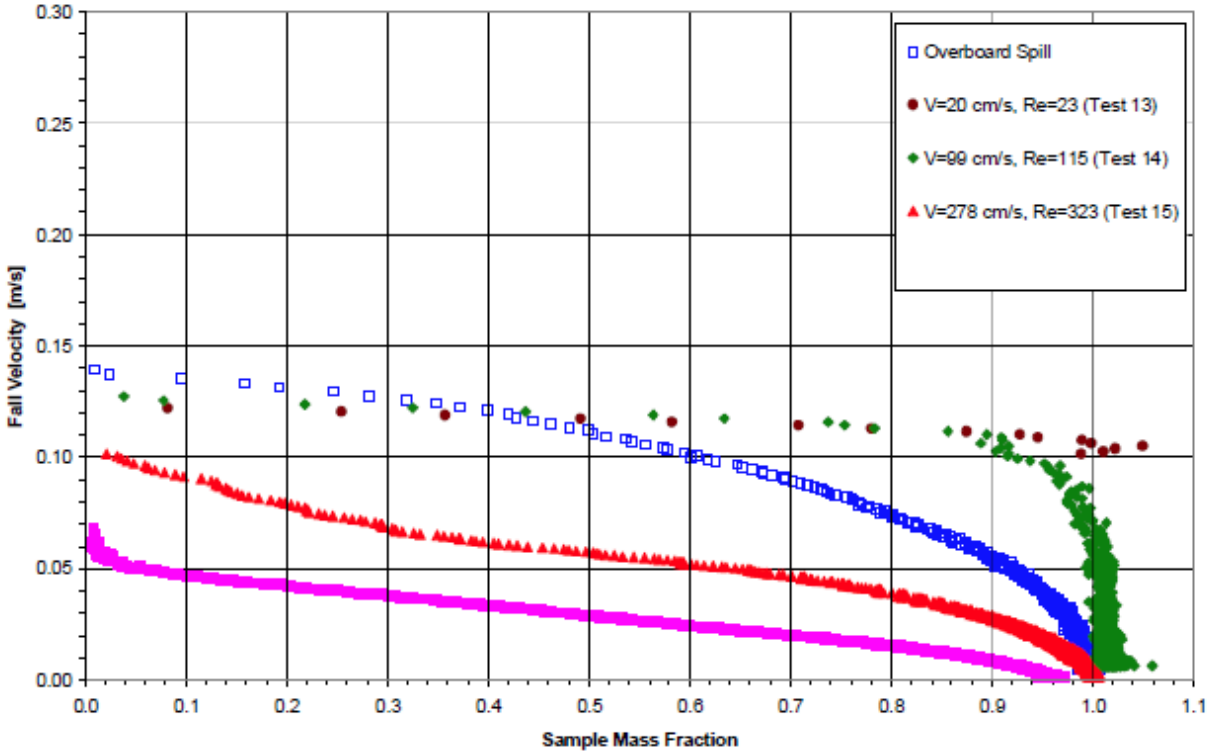


**Figure 3-10. Fall Velocity Distributions for Submerged Jet Case for Mud D (specific gravity 1.40) (From SwRI, 2007 Project No. 18.12210, 2007). Note that SwRI did not include a full legend, failing to reference to pink squares. While absent from the legend, these data were not required or included in the statistical analysis and therefore do not affect any results presented within this report.**

**Table 3-1. Drill cuttings fall velocities used for wide orifice, low speed (20 cm/s) jet simulations (SWRI, 2007).**

| Size Class | Sample Mass Fraction | Settling Velocity (20 cm/s simulation) | |
|---|---|---|---|
| | | cm/s | m/day |
| 1 | 0.1 | 12.2 | 10,540.8 |
| 2 | 0.1 | 12.2 | 10,540.8 |
| 3 | 0.1 | 12.0 | 10,368.0 |
| 4 | 0.1 | 11.9 | 10,281.6 |
| 5 | 0.1 | 11.7 | 10,108.8 |
| 6 | 0.1 | 11.4 | 9,849.6 |
| 7 | 0.1 | 11.3 | 9,763.2 |
| 8 | 0.1 | 11.2 | 9,676.8 |
| 9 | 0.1 | 10.8 | 9,331.2 |
| 10 | 0.1 | 10.3 | 8,899.2 |

**Table 3-2. Drill cuttings fall velocities used for narrow orifice, high speed (278 cm/s) jet simulations (SWRI, 2007).**

| Size Class | Sample Mass Fraction | Settling Velocity (278 cm/s simulation) | |
|---|---|---|---|
| | | cm/s | m/day |
| 1 | 0.1 | 5.8 | 5,011.2 |
| 2 | 0.1 | 4.2 | 3,628.8 |
| 3 | 0.1 | 4.0 | 3,456.0 |
| 4 | 0.1 | 3.5 | 3,024.0 |
| 5 | 0.1 | 3.2 | 2,764.8 |
| 6 | 0.1 | 2.8 | 2,419.2 |
| 7 | 0.1 | 2.2 | 1,900.8 |
| 8 | 0.1 | 1.8 | 1,555.2 |
| 9 | 0.1 | 1.3 | 1,123.2 |
| 10 | 0.1 | 0.8 | 691.2 |

# 4 Model Results

The fate of mud and cuttings released from operational drilling activities at Site 1 and Site 2 were assessed using deterministic scenarios corresponding to the drilling period and discharge volumes shown in Table 2-2. For both sites, three deterministic simulations of different jet sizes, speeds, and release locations were performed during two current regimes (representative of fall and winter), totalling twelve simulations. MUDMAP was used to model the trajectory of SBM particles from accidental release simulations and to track the far field dispersion for a minimum of 6 hours after the release, accounting for the prolonged settling of very fine mud particles from the water column. Based off the depth, and settling velocities of the muds, 6 hours is sufficient to allow for all particles to reach the seabed. Surface releases were simulated with settling velocities derived from low speed jet releases and therefore have faster settling velocities, reaching the seabed within approximately 2-4 hours (for deepest site). Riser flex join failures were simulated approximately 20 m above the seafloor and have slower settling velocities as a result of the high speed jet release, but still reach the seabed within first 2 hours, due to the short distance to fall. The output of MUDMAP simulations are concentration grids that describes loading to the water column and seabed associated with each accidental release simulation.

## 4.1 Predicted Seabed Deposition

MUDMAP was used to predict seabed deposition at Site 1 and Site 2 from potential accidental releases of SBM for each scenario summarized in Table 2-2.

- Figure 4-1 to Figure 4-12 present seabed deposition associated with the release of each of the accidental SBM release simulations described above,
- Table 4-1 and Table 4-2 summarize the areal extent of seabed deposition resulting from the modelled releases, and
- Table 4-3 and Table 4-4 summarize the maximum distance seabed deposition extends from the release sites.

### 4.1.1 Site 1 Release (Seabed Deposition)

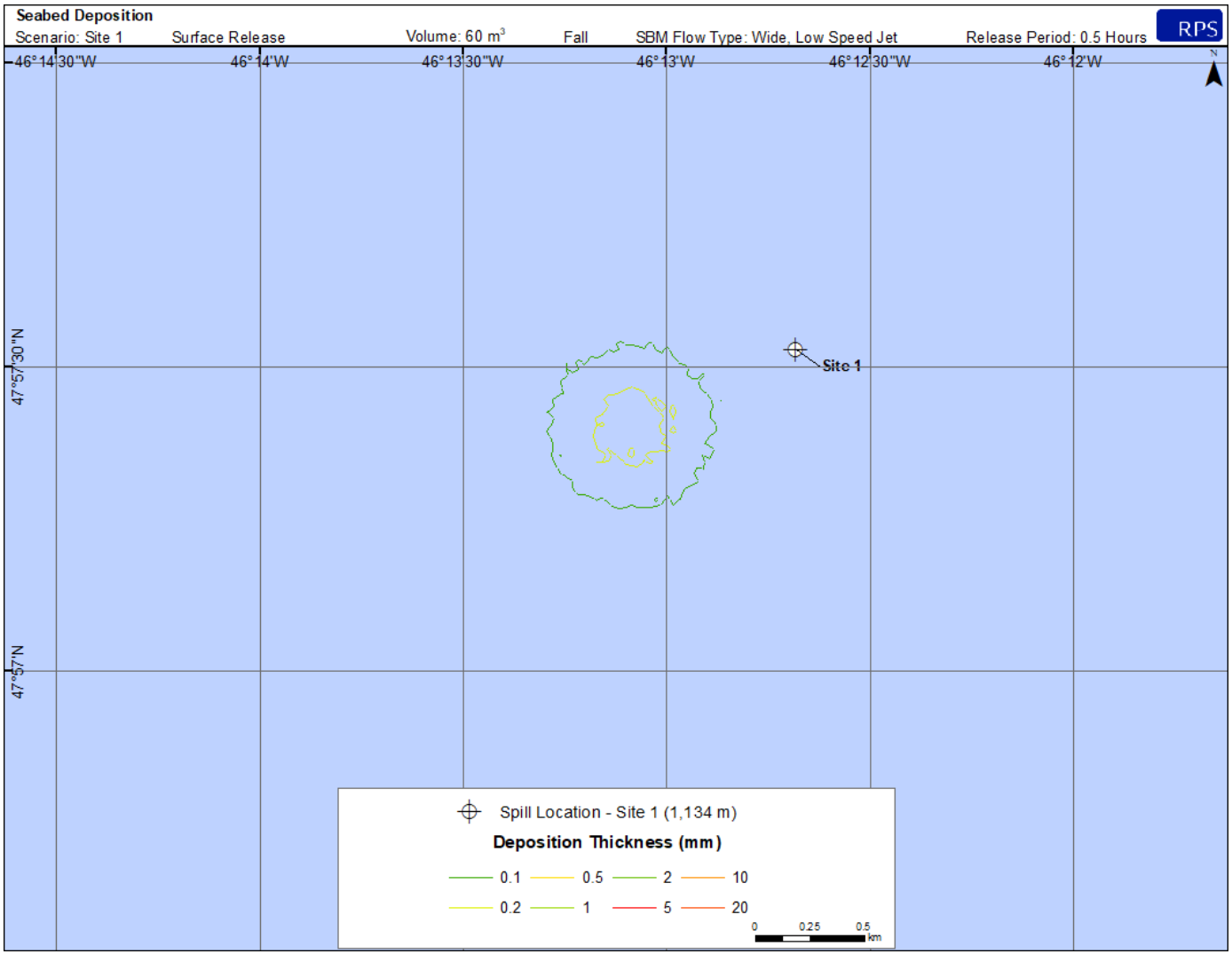


**Figure 4-1. Predicted thickness from an accidental surface release of 60 m³ at the Site 1 release site (Fall).**

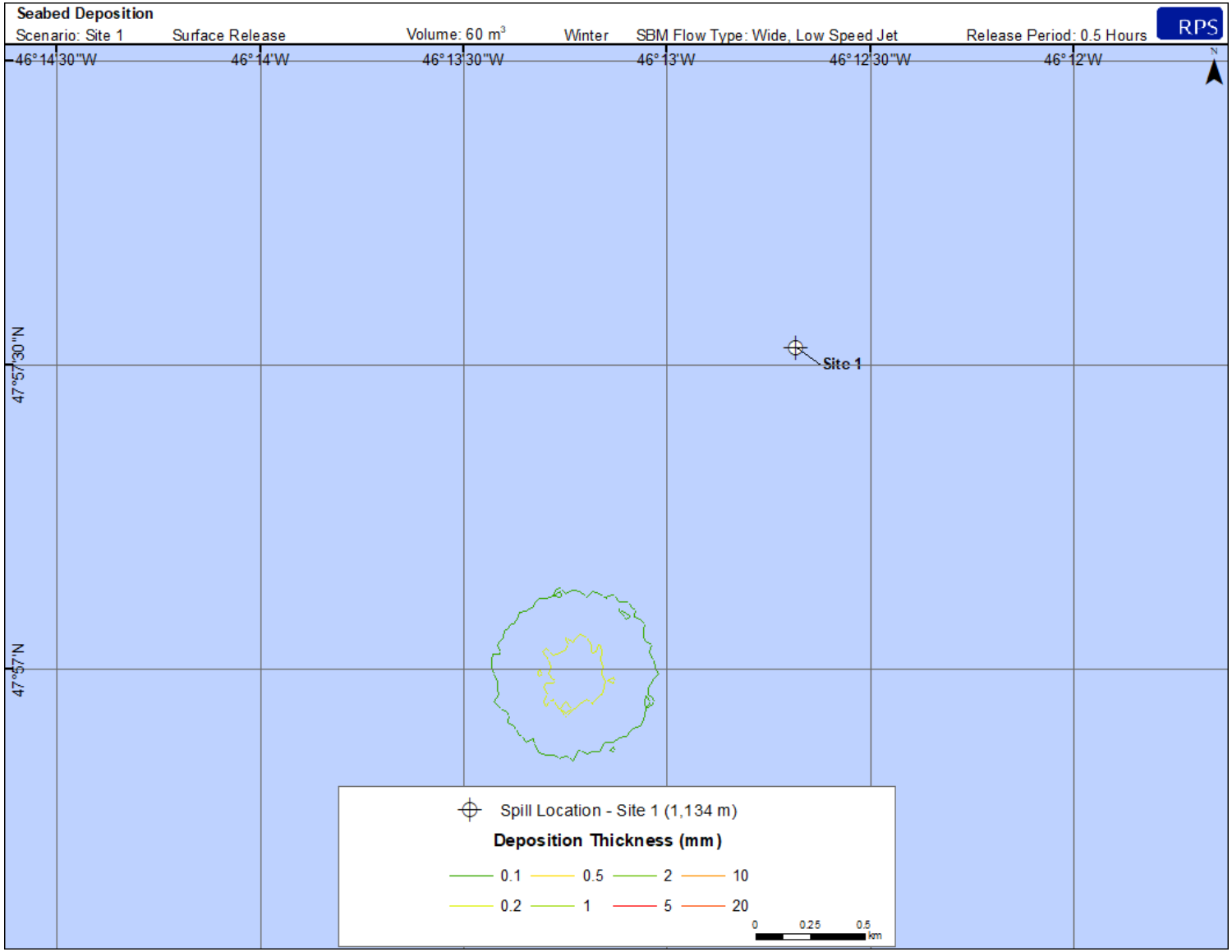


**Figure 4-2. Predicted thickness from an accidental surface release of 60 m³ at the Site 1 release site (Winter).**

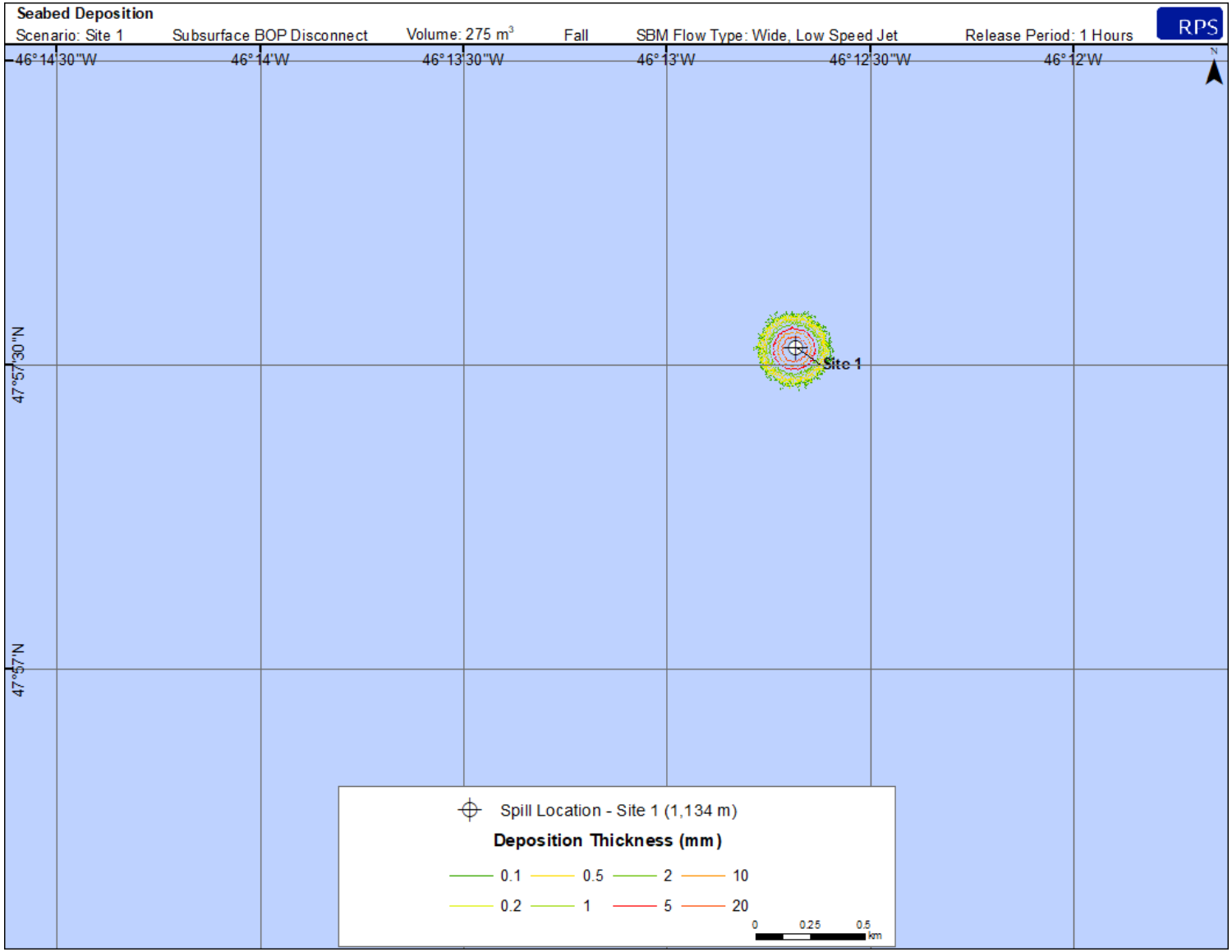


**Figure 4-3. Predicted thickness from a flex joint failure accidental seabed release 275 m$^3$ at the Site 1 release site (Fall).**

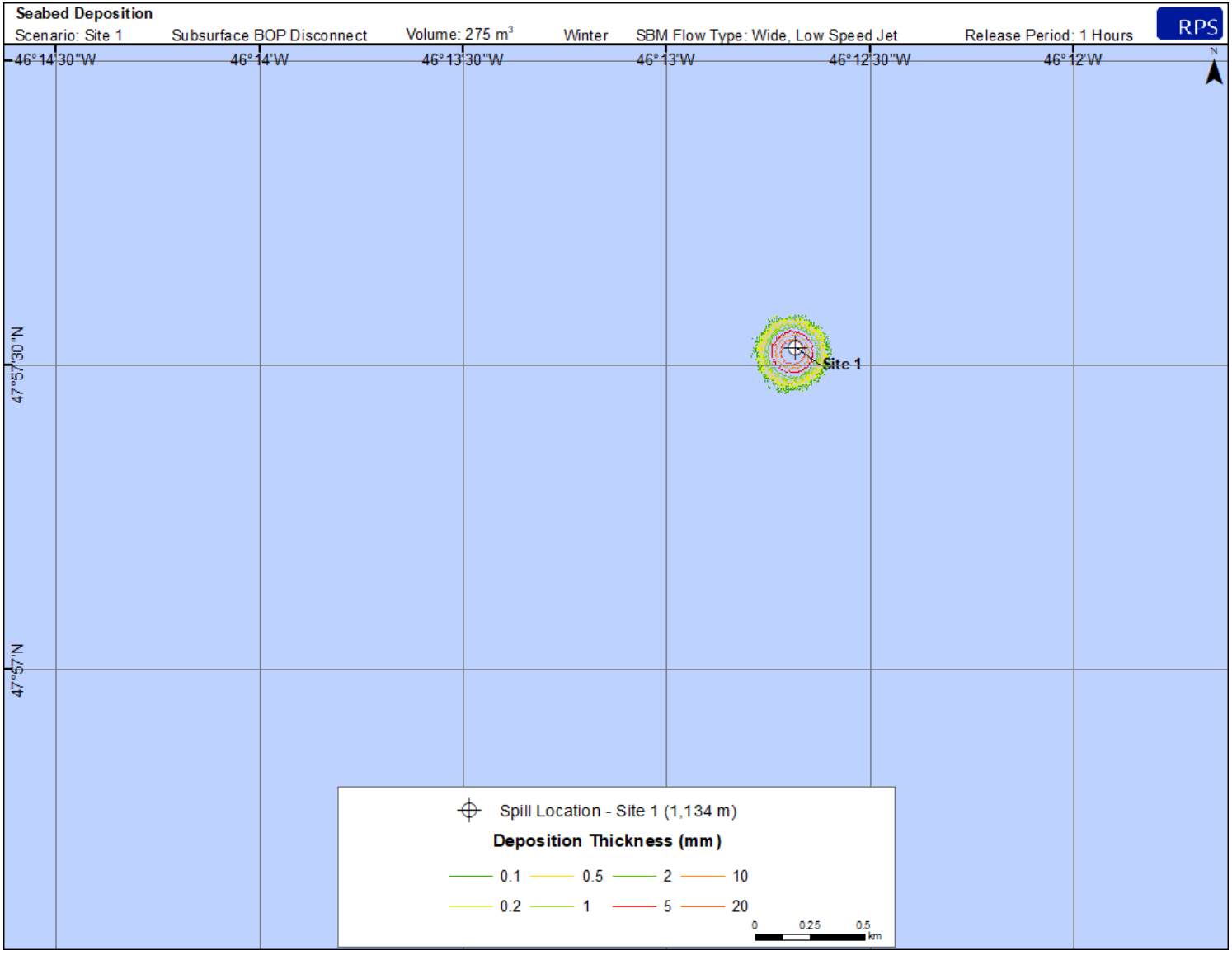


**Figure 4-4. Predicted thickness from a flex joint failure accidental seabed release 275 m$^3$ at the Site 1 release site (Winter).**

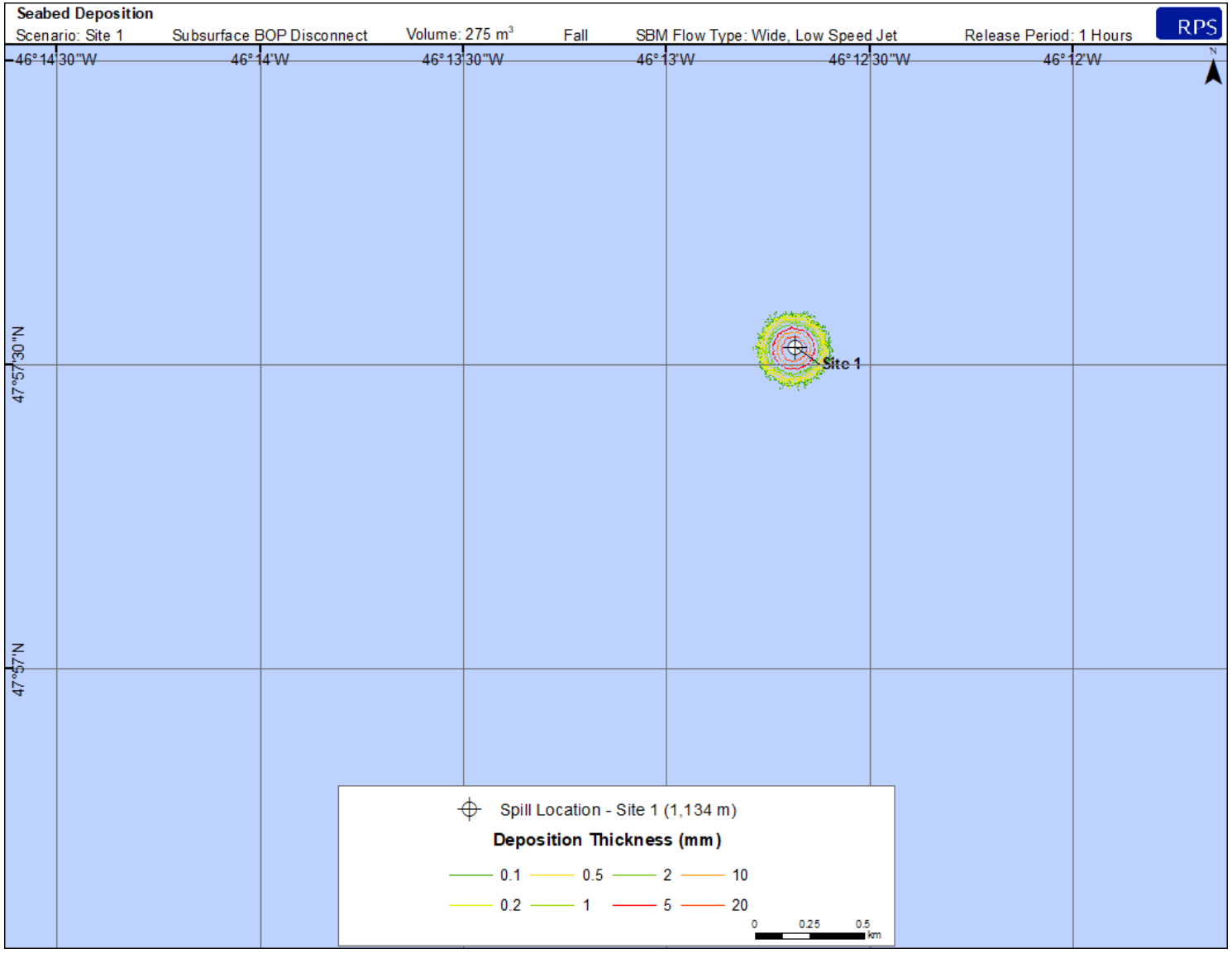


**Figure 4-5. Predicted thickness from a BOP disconnect accidental seabed release 275 m$^3$ at the Site 1 release site (Fall).**

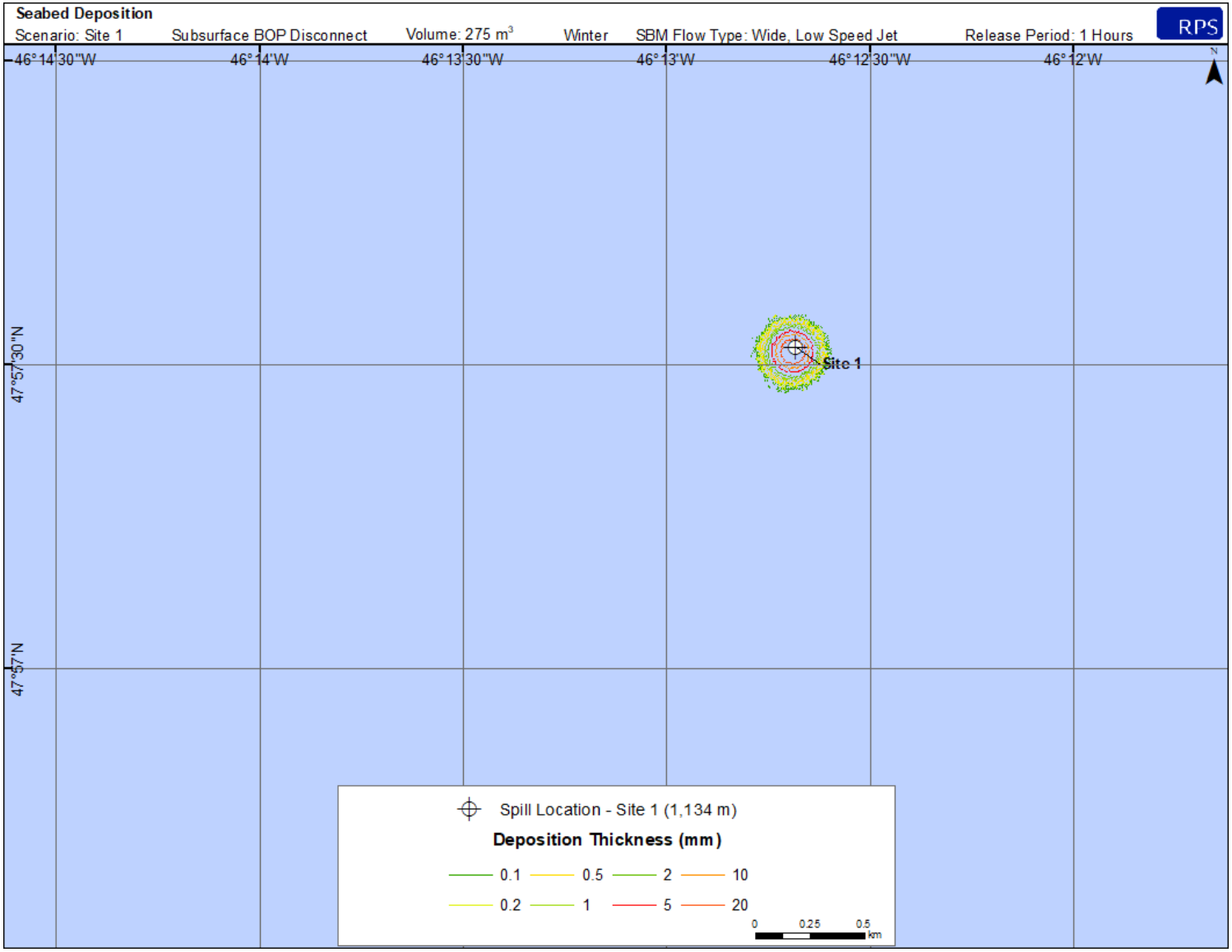


**Figure 4-6. Predicted thickness from a BOP disconnect accidental seabed release 275 $m^3$ at the Site 1 release site (Winter).**

### 4.1.2 Site 2 Release Site (Seabed Deposition)

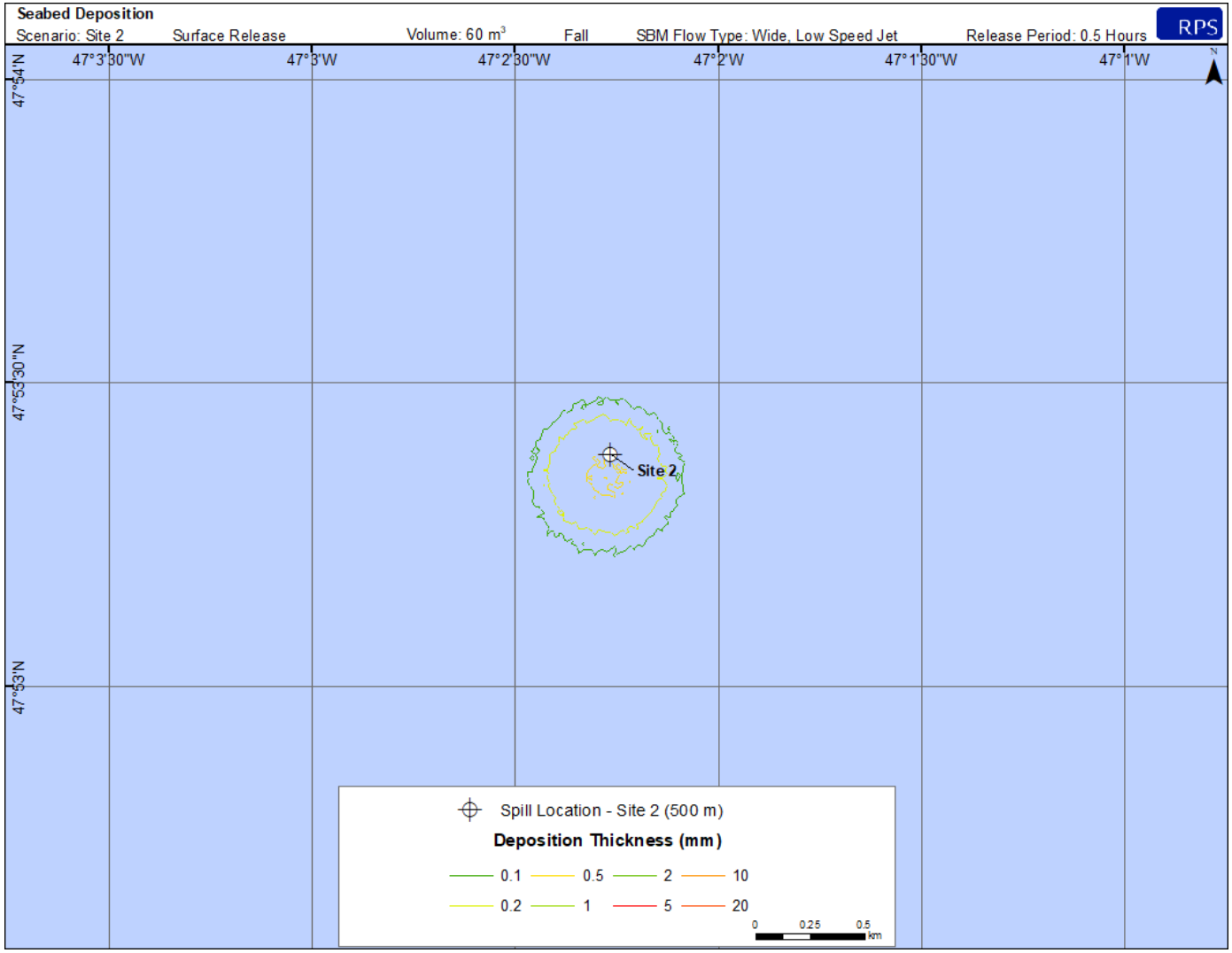


**Figure 4-7. Predicted thickness from an accidental surface release of 60 m$^3$ at the Site 2 release site (Fall).**

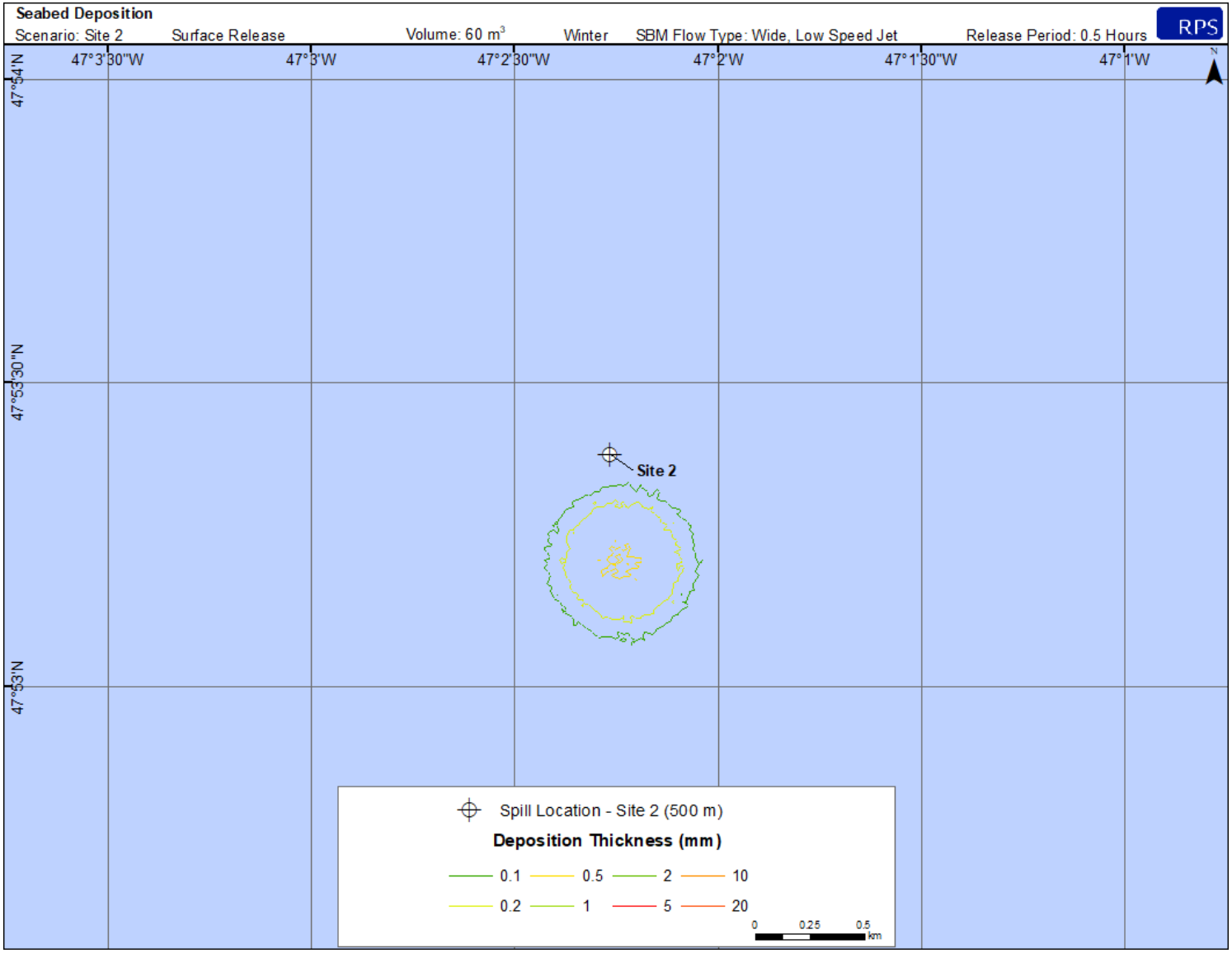


**Figure 4-8. Predicted thickness from an accidental surface release of 60 $m^3$ at the Site 2 release site (Winter).**

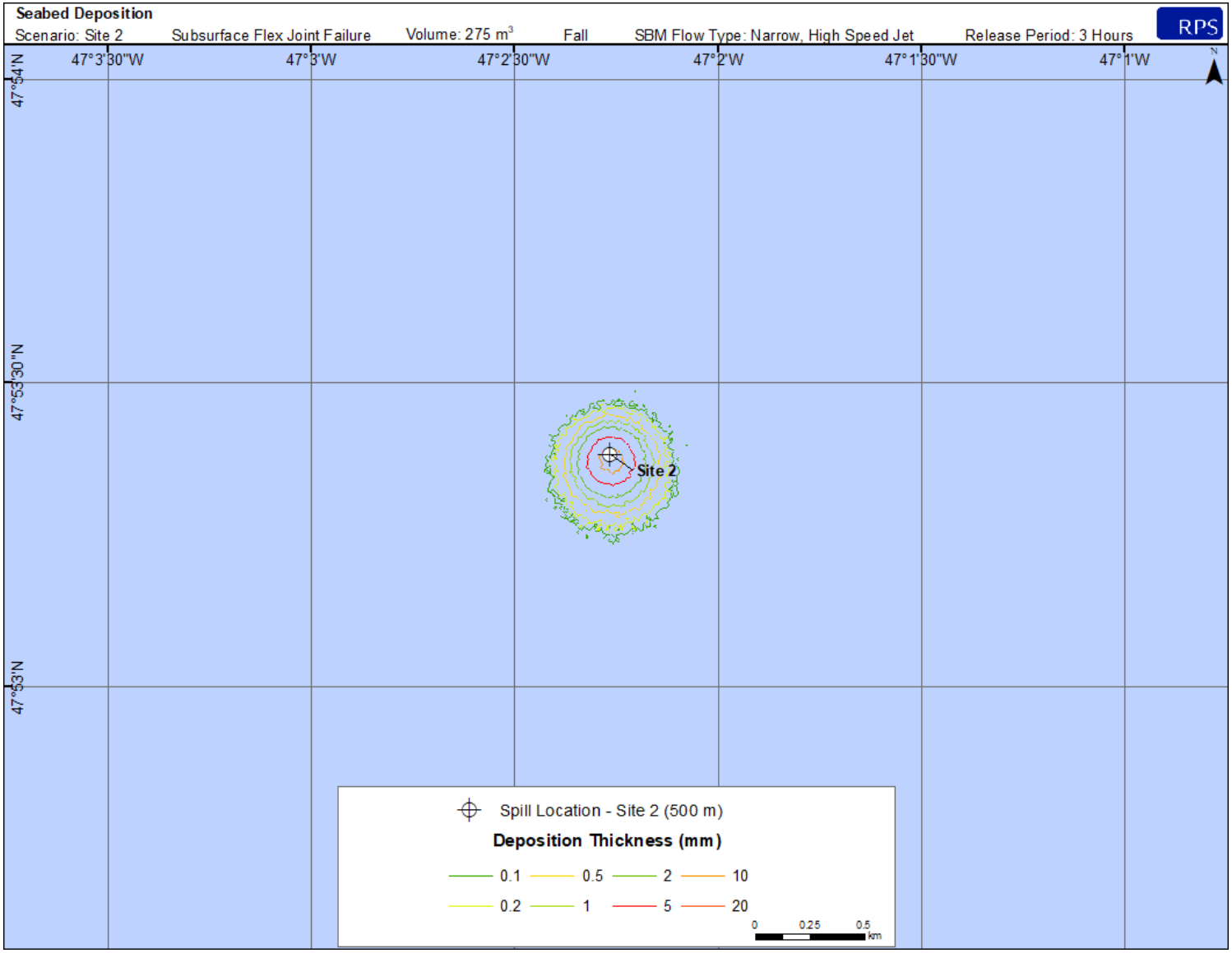


**Figure 4-9. Predicted thickness from a flex joint failure accidental seabed release 275 m$^3$ at the Site 2 release site (Fall).**

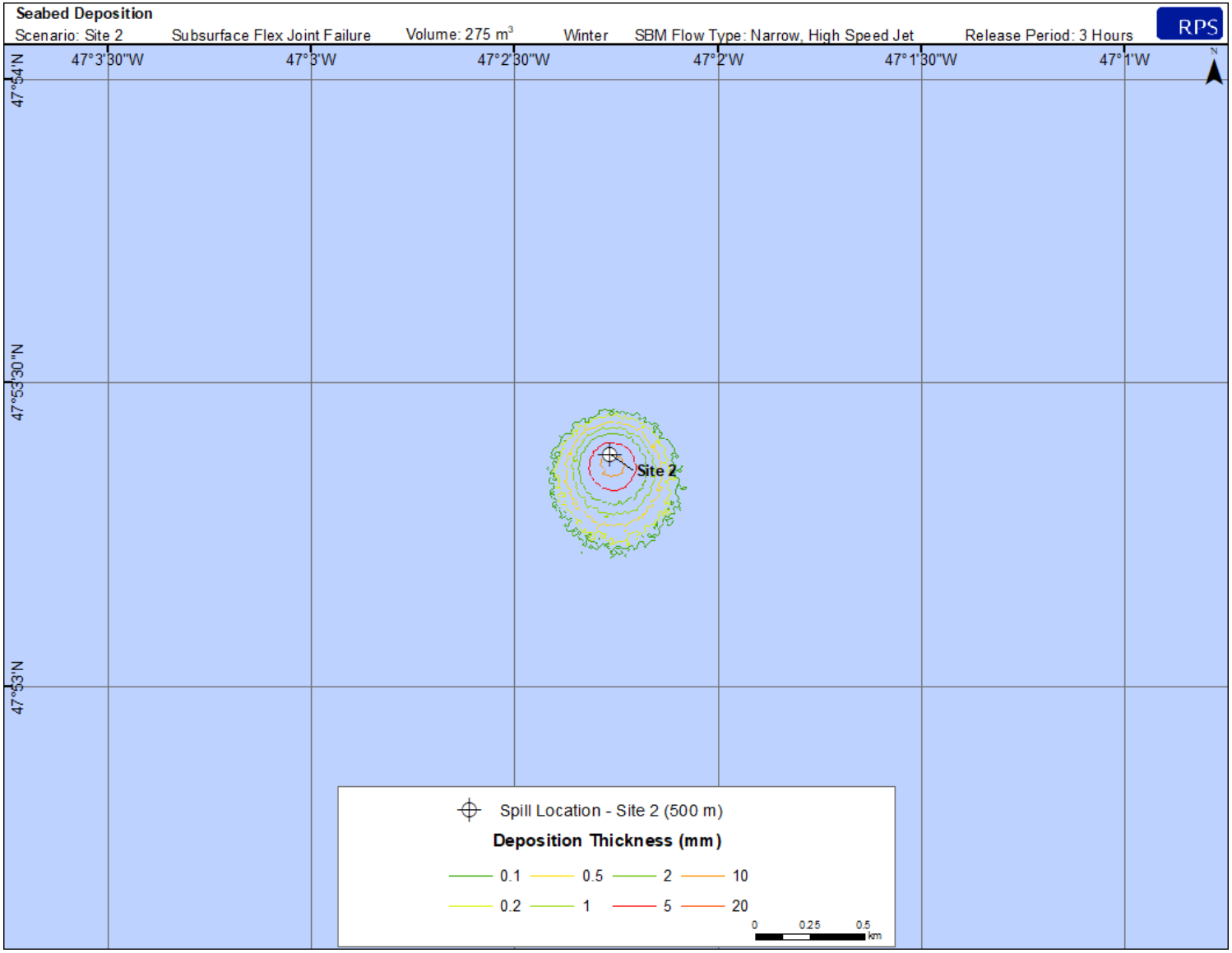


**Figure 4-10. Predicted thickness from a flex joint failure accidental seabed release 275 m$^3$ at the Site 2 release site (Winter).**

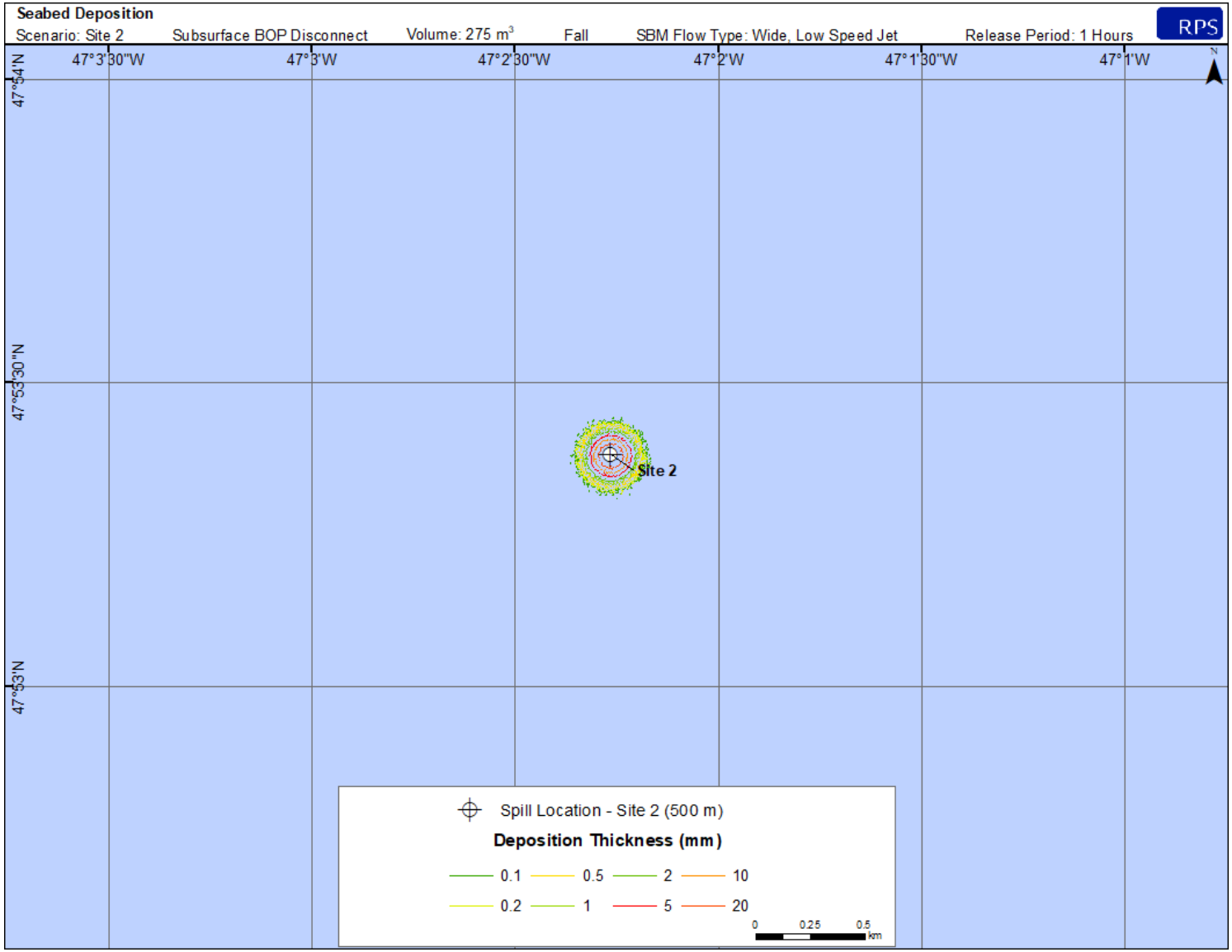


**Figure 4-11. Predicted thickness from a BOP disconnect accidental seabed release 275 m³ at Site 2 release site (Fall).**

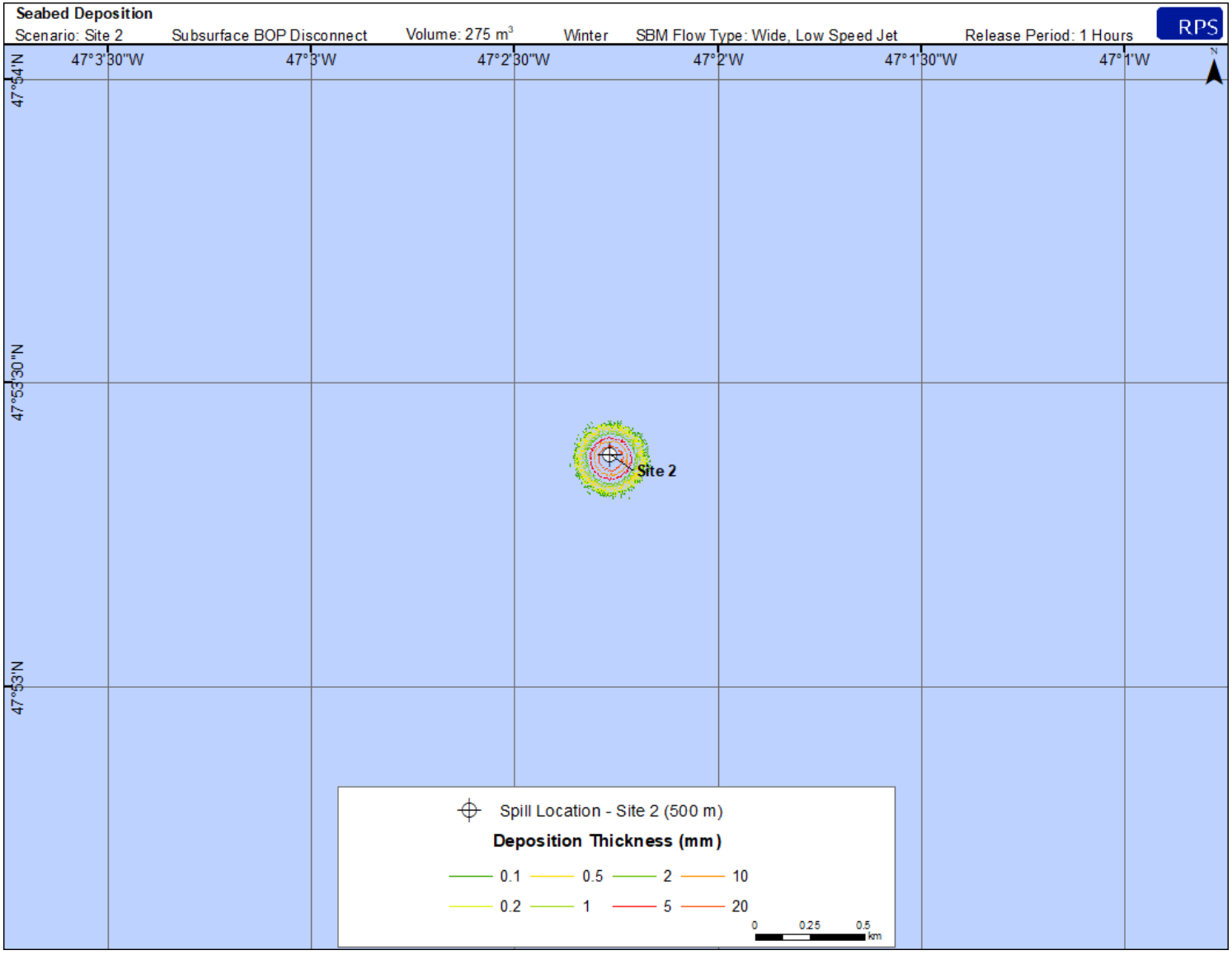


**Figure 4-12. Predicted thickness from a BOP disconnect accidental seabed release 275 $m^3$ at the Site 2 release site (Winter).**

### 4.1.3 Summary of Predicted Seabed Deposition

**Table 4-1. Areal extent of seabed deposition (by thickness interval) for Site 1 simulations.**

| Deposition Thickness (mm) | Cumulative Area Exceeding ($km^2$) | | | | | |
|---|---|---|---|---|---|---|
| | Surface Tank Spill (Fall) | Surface Tank Spill (Winter) | Flex Joint Failure (Fall) | Flex Joint Failure (Winter) | Subsea BOP Disconnect (Fall) | Subsea BOP Disconnect (Winter) |
| **0.1** | **0.19647** | **0.19314** | **0.12188** | **0.1301** | **0.03533** | **0.03557** |
| 0.2 | 0.03834 | 0.03125 | 0.09884 | 0.10587 | 0.03204 | 0.03202 |
| 0.5 | 0 | 0 | 0.07035 | 0.07333 | 0.02596 | 0.02611 |
| **1** | **0** | **0** | **0.0511** | **0.05233** | **0.02165** | **0.02198** |
| 2 | 0 | 0 | 0.03427 | 0.03463 | 0.01778 | 0.01783 |
| 5 | 0 | 0 | 0.01596 | 0.01503 | 0.01215 | 0.01222 |
| **10** | **0** | **0** | **0.00428** | **0.00343** | **0.0081** | **0.00814** |
| 20 | 0 | 0 | 0 | 0 | 0.00426 | 0.00428 |

**Table 4-2. Areal extent of seabed deposition (by thickness interval) for Site 2 simulations.**

| Deposition Thickness (mm) | Cumulative Area Exceeding ($km^2$) | | | | | |
|---|---|---|---|---|---|---|
| | Surface Tank Spill (Fall) | Surface Tank Spill (Winter) | Flex Joint Failure (Fall) | Flex Joint Failure (Winter) | Subsea BOP Disconnect (Fall) | Subsea BOP Disconnect (Winter) |
| **0.1** | **0.16856** | **0.16823** | **0.12602** | **0.13114** | **0.03549** | **0.03525** |
| 0.2 | 0.09827 | 0.09815 | 0.09858 | 0.10378 | 0.03212 | 0.03226 |
| 0.5 | 0.00838 | 0.00602 | 0.06827 | 0.07189 | 0.02576 | 0.02585 |
| **1** | **0** | **0** | **0.05106** | **0.05145** | **0.02174** | **0.02187** |
| 2 | 0 | 0 | 0.03428 | 0.0343 | 0.01778 | 0.01785 |
| 5 | 0 | 0 | 0.01606 | 0.01598 | 0.01214 | 0.01219 |
| **10** | **0** | **0** | **0.00396** | **0.00372** | **0.00809** | **0.00824** |
| 20 | 0 | 0 | 0 | 0 | 0.00424 | 0.00419 |

**Table 4-3. Maximum distance of thickness contours (distance from release site) for Site 1 (Site 1) simulations.**

| Deposition Thickness (mm) | Maximum extent from release site (km) | | | | | |
|---|---|---|---|---|---|---|
| | Surface Tank Spill (Fall) | Surface Tank Spill (Winter) | Flex Joint Failure (Fall) | Flex Joint Failure (Winter) | Subsea BOP Disconnect (Fall) | Subsea BOP Disconnect (Winter) |
| 0.1 | 0.81 | 1.46 | 0.29 | 0.36 | 0.14 | 0.15 |
| 1 | 0 | 0 | 0.17 | 0.22 | 0.1 | 0.11 |
| 10 | 0 | 0 | 0.06 | 0.08 | 0.06 | 0.07 |

**Table 4-4. Maximum distance of thickness contours (distance from release site) for Site 2 (Site 2) simulations.**

| Deposition Thickness (mm) | Maximum extent from release site (km) | | | | | |
|---|---|---|---|---|---|---|
| | Surface Tank Spill (Fall) | Surface Tank Spill (Winter) | Flex Joint Failure (Fall) | Flex Joint Failure (Winter) | Subsea BOP Disconnect (Fall) | Subsea BOP Disconnect (Winter) |
| 0.1 | 0.32 | 0.59 | 0.28 | 0.35 | 0.14 | 0.15 |
| 1 | 0 | 0 | 0.16 | 0.2 | 0.1 | 0.1 |
| 10 | 0 | 0 | 0.06 | 0.07 | 0.06 | 0.07 |

## 4.2 Predicted Water Column Concentrations

MUDMAP was also used to evaluate concentrations of total suspended solids (TSS) in the water column as a result of accidental releases of SBM for the twelve scenarios summarized in Table 2-2.

- Figure 4-13 through Figure 4-36 present maximum water column concentrations associated with the release of each accidental SBM release simulations described above. Each figure pair includes a top-down view as well as a cross-section of the release. These figures do not represent any instantaneous snapshot of water column concentrations, but instead depict the maximum, time-integrated TSS within the study domain for each modelled release,
- Table 4-5 and Table 4-6 summarize the areal extent of water column concentrations resulting from the modelled releases, and
- Table 4-7 and Table 4-8 summarize the maximum distance water column concentrations extend from the release sites.

### 4.2.1 Site 1 Release Site (Water Column Concentrations)

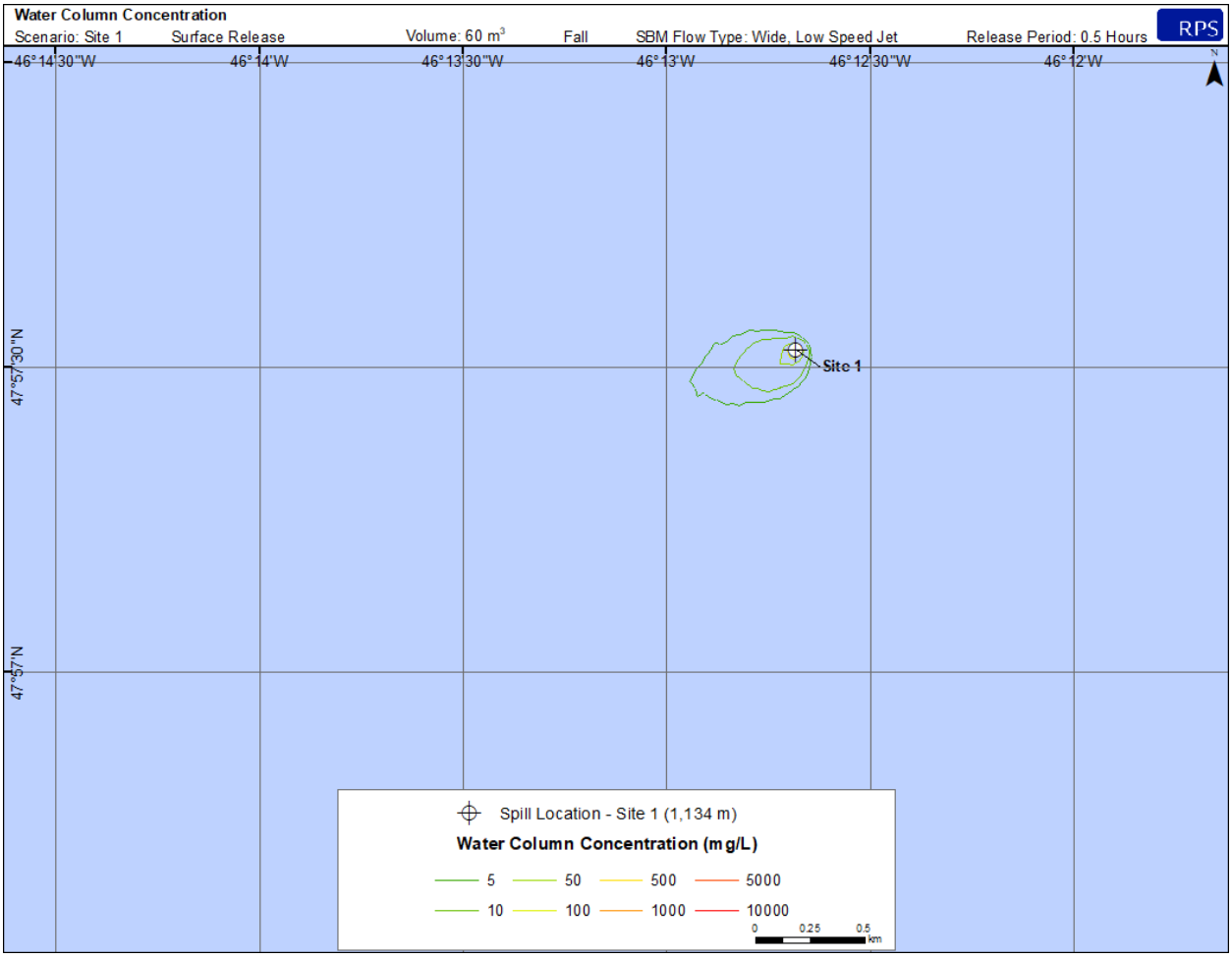


**Figure 4-13. Predicted water column concentration from an accidental surface release of 60 m$^3$ at Site 1 release site (Fall).**

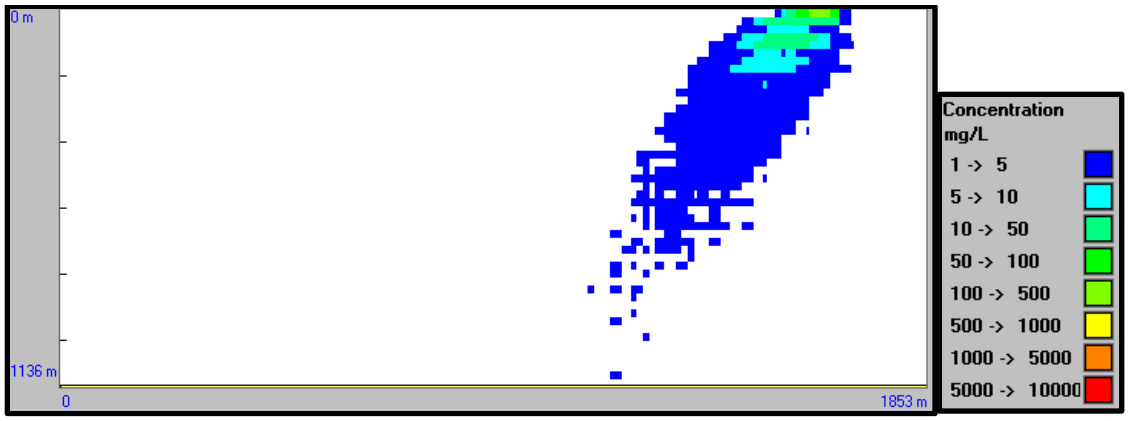


**Figure 4-14. Cross sectional view of predicted water column concentration from an accidental surface release of 60 m$^3$ at Site 1 release site (Fall).**

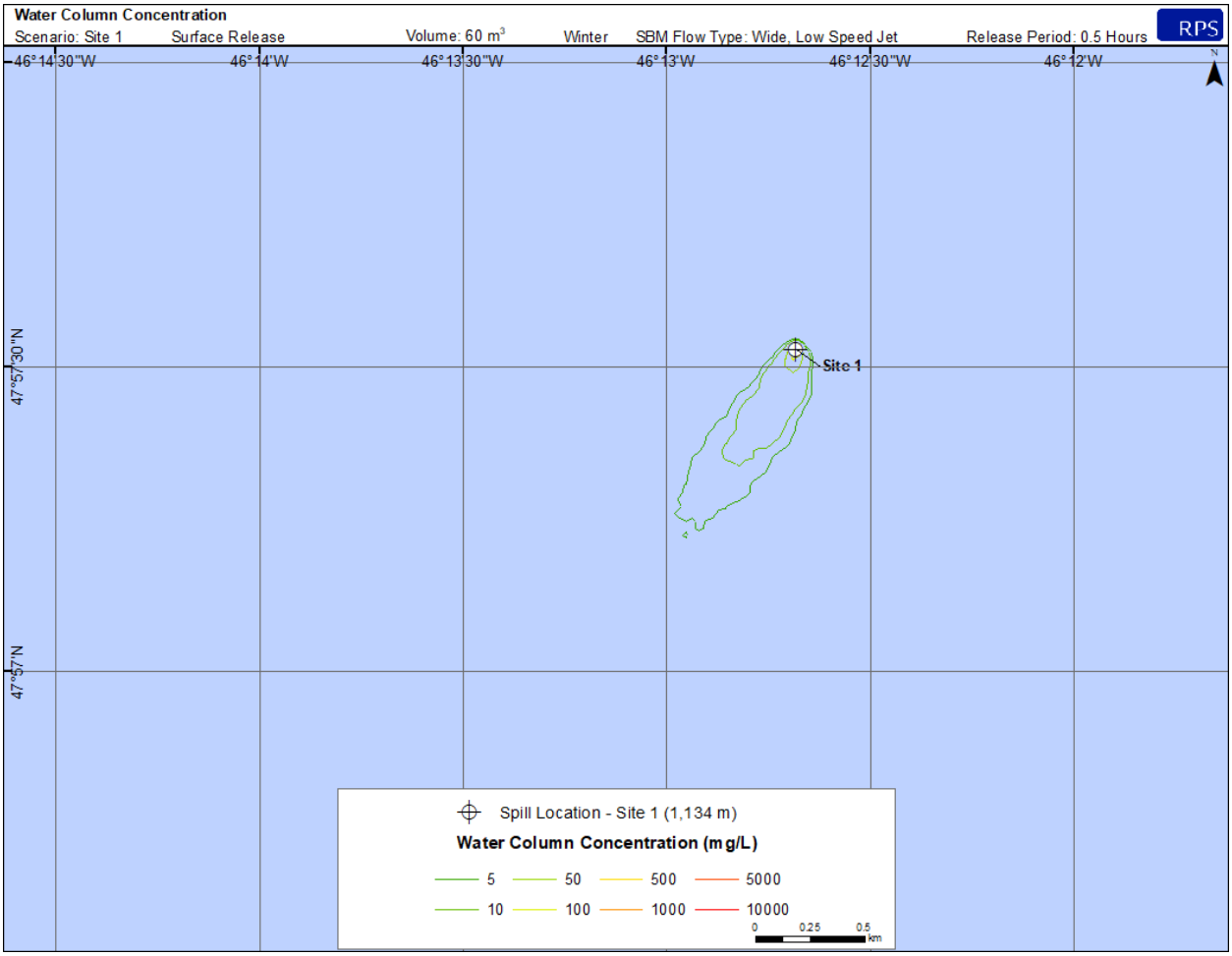


**Figure 4-15. Predicted water column concentration from an accidental surface release of 60 m$^3$ at Site 1 release site (Winter).**

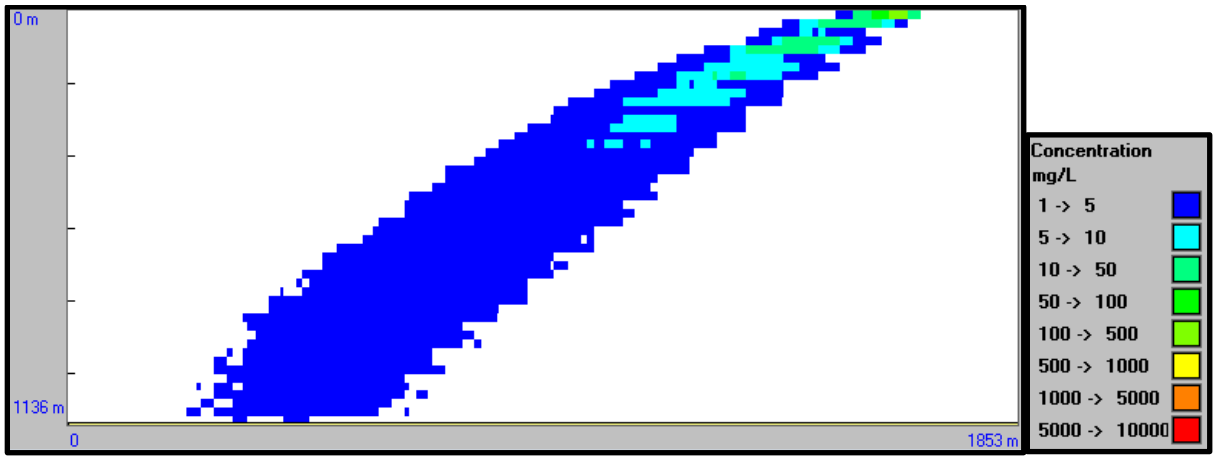


**Figure 4-16. Cross sectional view of predicted water column concentration from an accidental surface release of 60 m$^3$ at Site 1 release site (Winter).**

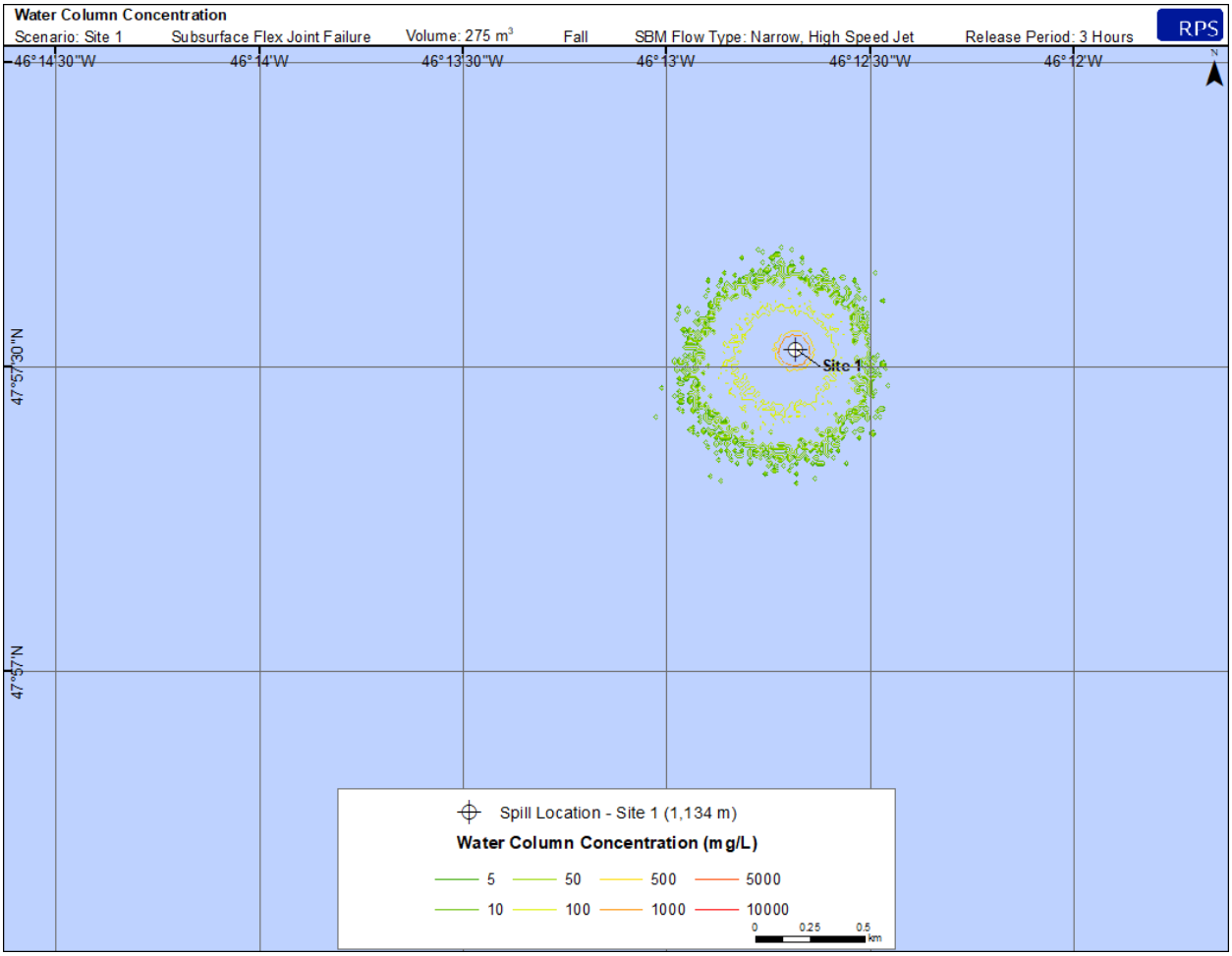


**Figure 4-17. Predicted water column concentration from a flex joint failure accidental seabed release 275 m$^3$ at Site 1 release site (Fall).**

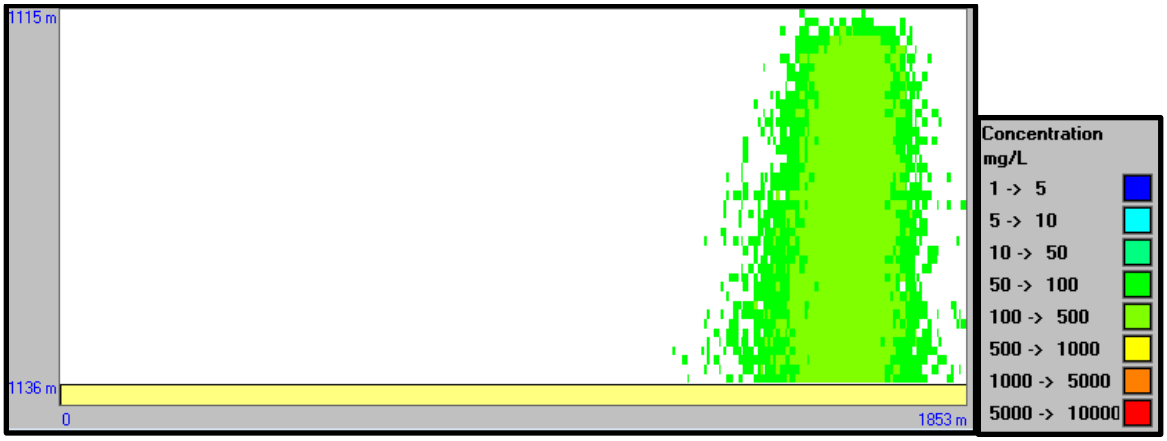


**Figure 4-18. Cross sectional view of predicted water column concentration from a flex joint failure accidental seabed release 275 m$^3$ at Site 1 release site (Fall).**

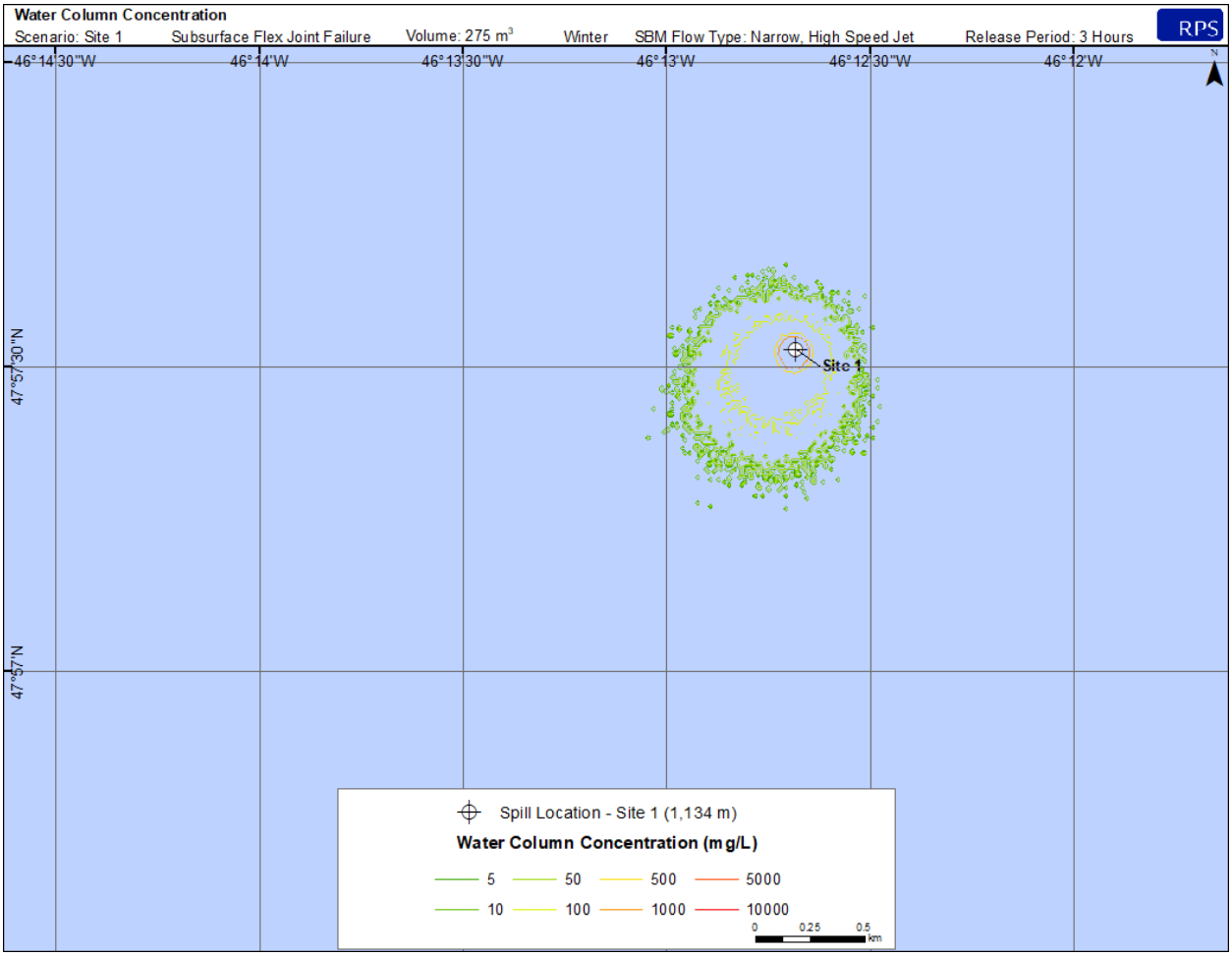


**Figure 4-19. Predicted water column concentration from a flex joint failure accidental seabed release 275 m$^3$ at Site 1 release site (Winter).**

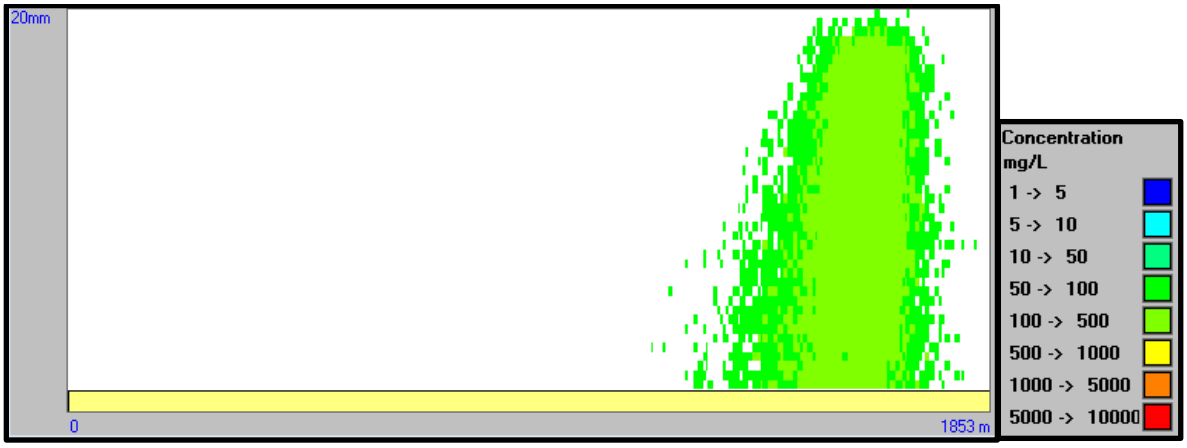


**Figure 4-20. Cross sectional view of predicted water column concentration from a flex joint failure accidental seabed release 275 m$^3$ at Site 1 release site (Winter).**

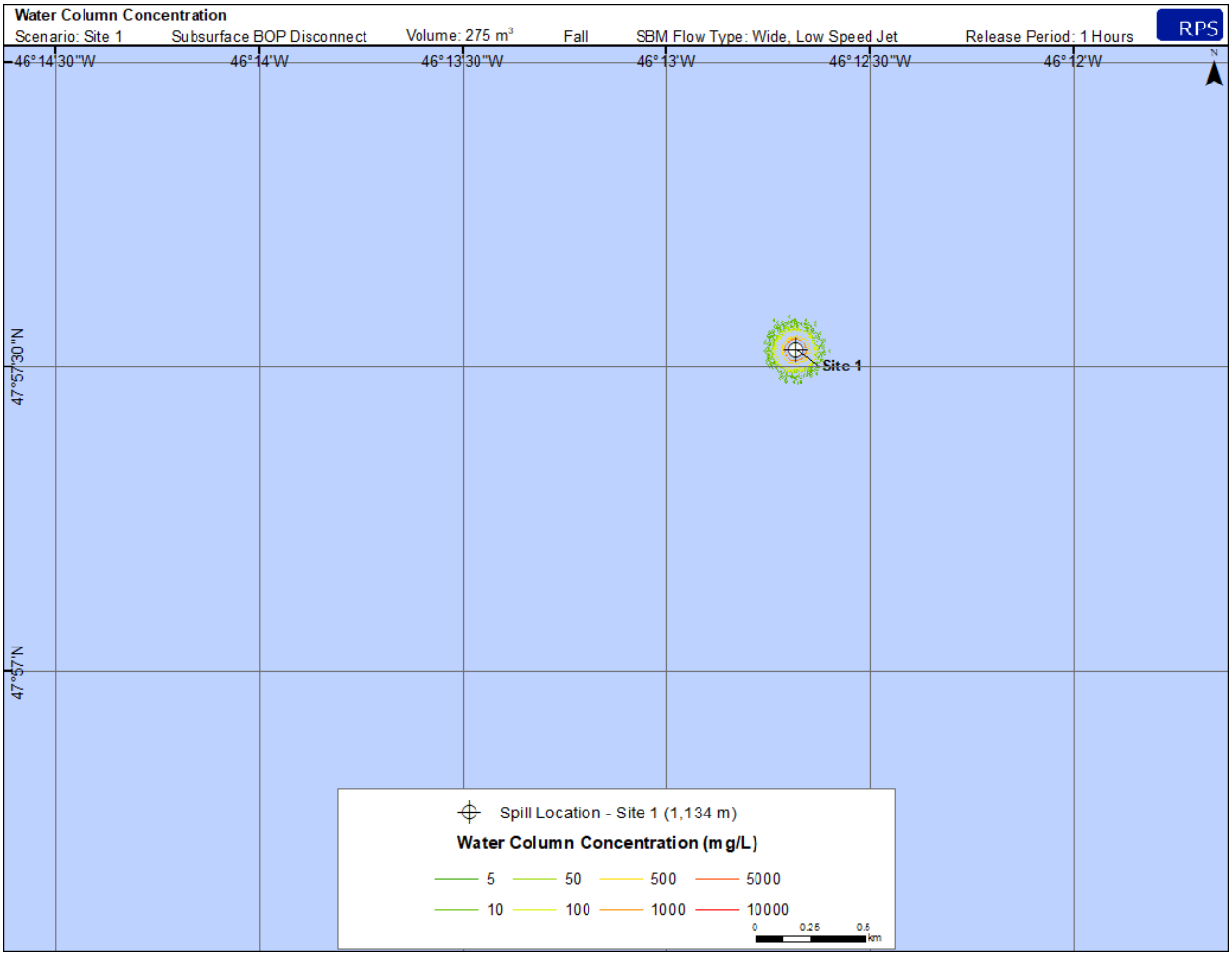


**Figure 4-21. Predicted water column concentration from a BOP disconnect accidental seabed release 275 m$^3$ at Site 1 release site (Fall).**

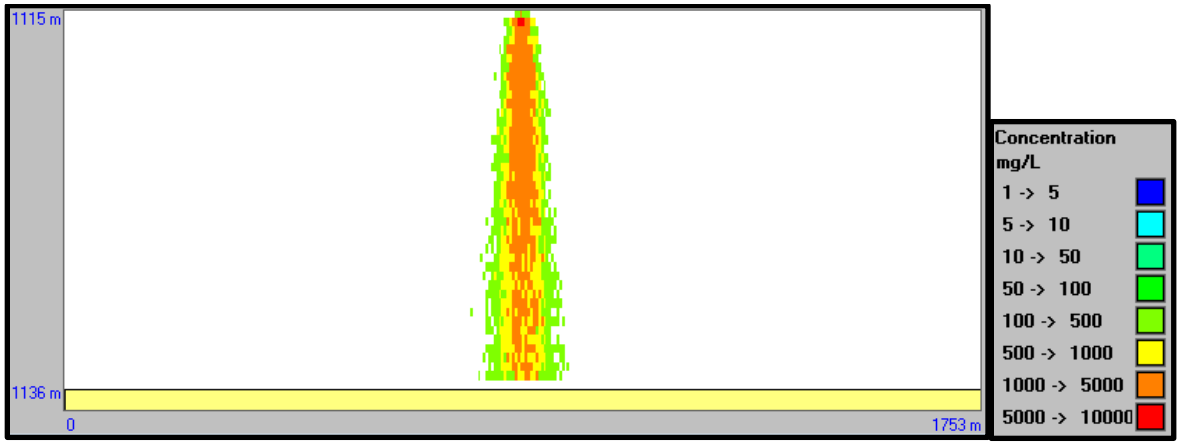


**Figure 4-22. Predicted water column concentration from a BOP disconnect accidental seabed release 275 m$^3$ at Site 1 release site (Fall).**

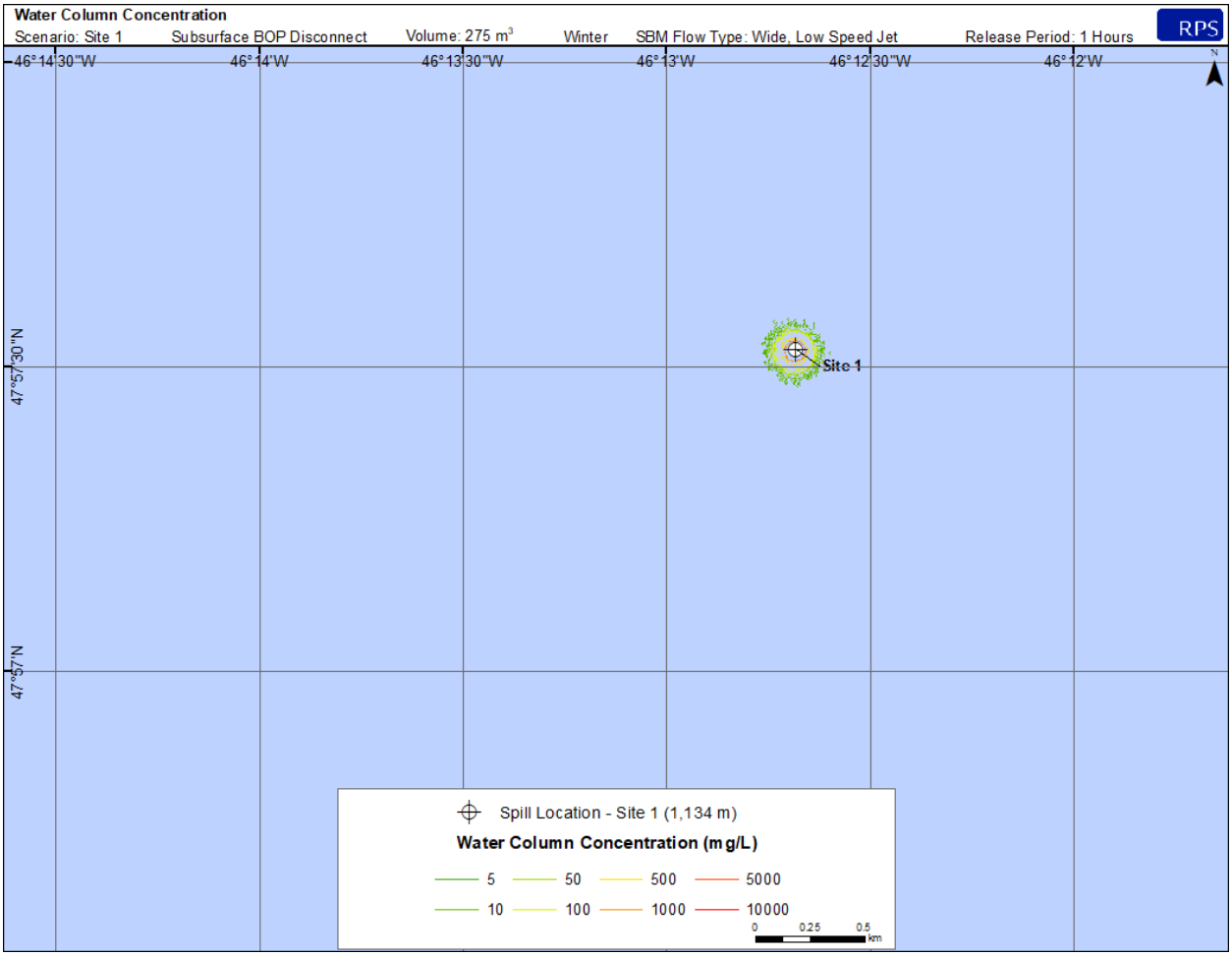


**Figure 4-23. Predicted water column concentration from a BOP disconnect accidental seabed release 275 m$^3$ at Site 1 release site (Winter).**

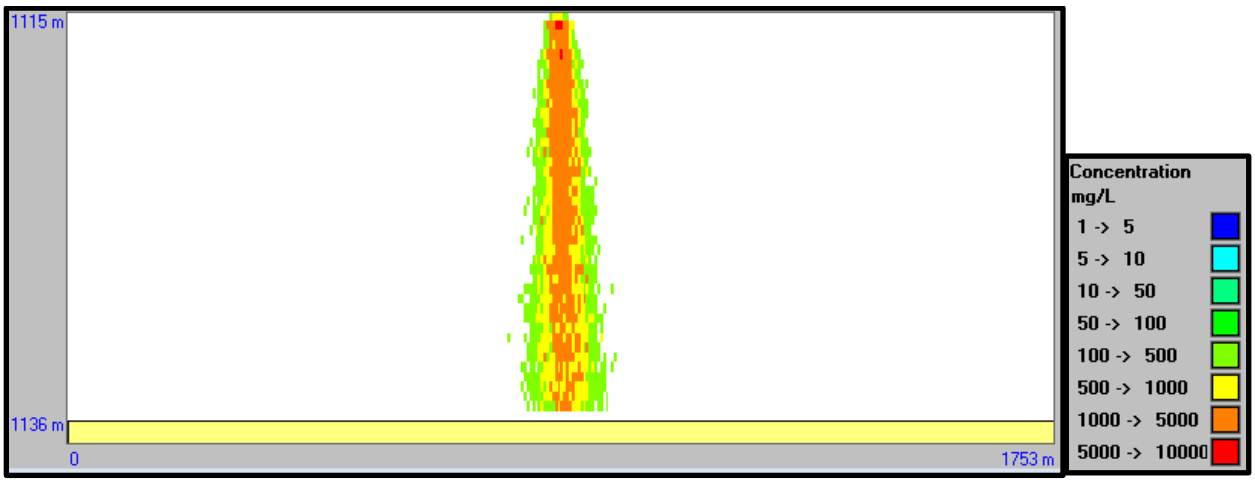


**Figure 4-24. Cross sectional view of predicted water column concentration from a BOP disconnect accidental seabed release 275 m$^3$ at Site 1 release site (Winter).**

### 4.2.2 Site 2 Release Site (Water Column Concentrations)

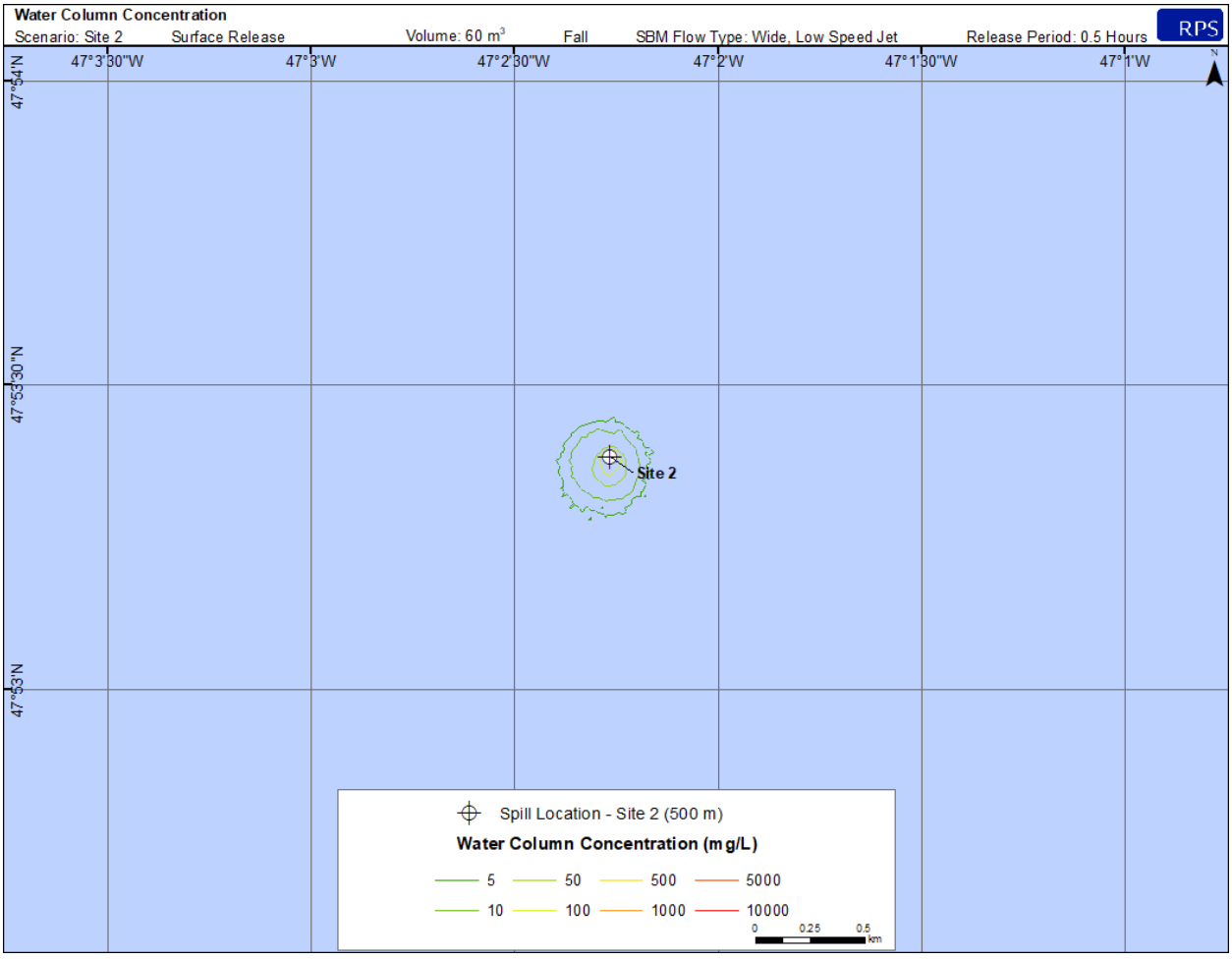


**Figure 4-25. Predicted water column concentration from an accidental surface release of 60 m$^3$ at Site 2 release site (Fall).**

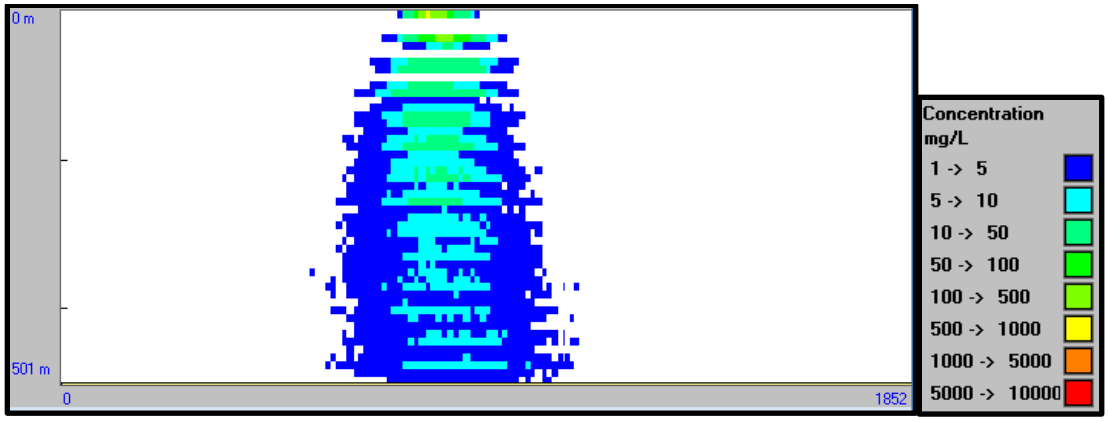


**Figure 4-26. Cross sectional view of predicted water column concentration from an accidental surface release of 60 m$^3$ at Site 2 release site (Fall).**

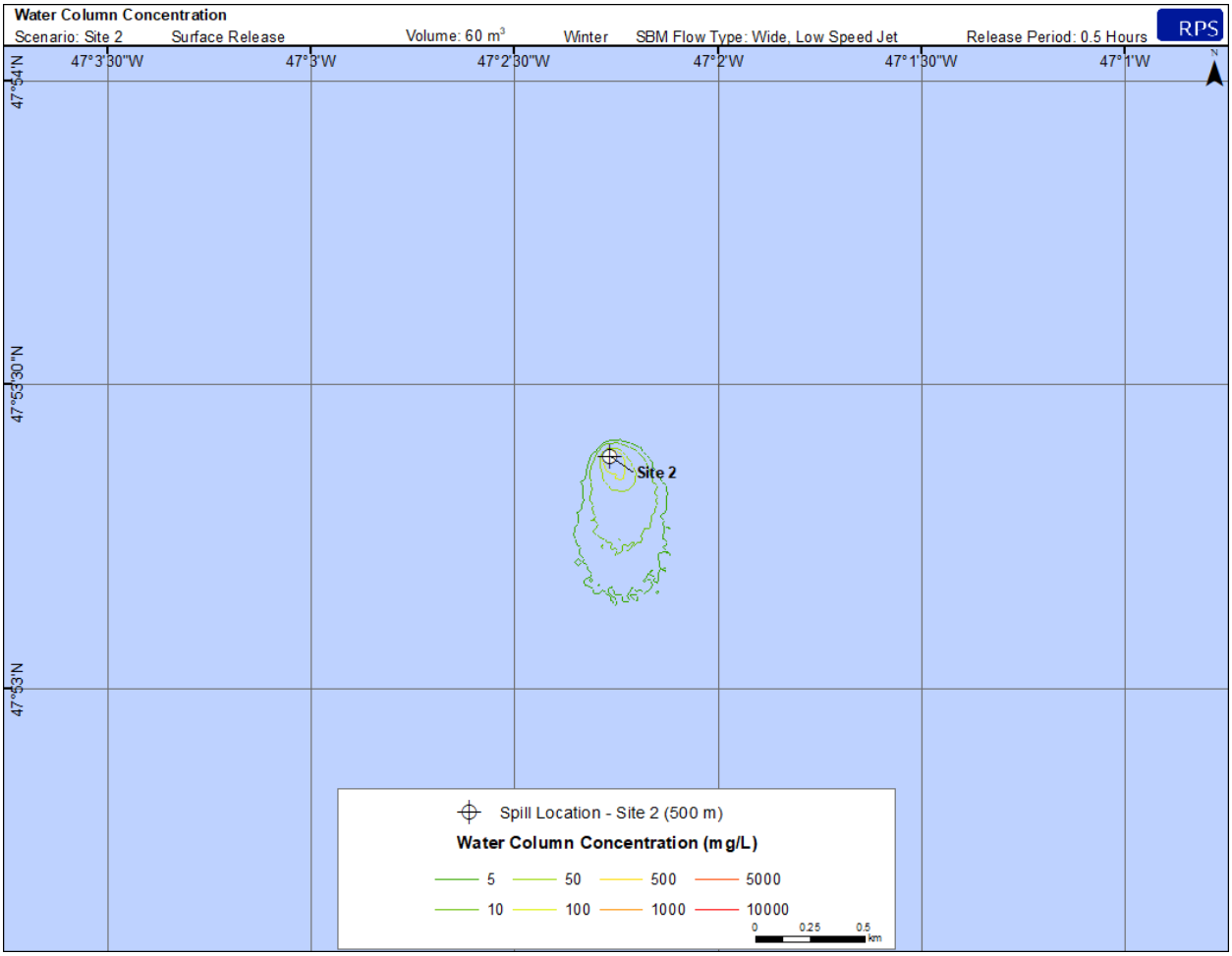


**Figure 4-27. Predicted water column concentration from an accidental surface release of 60 m$^3$ at Site 2 release site (Winter).**

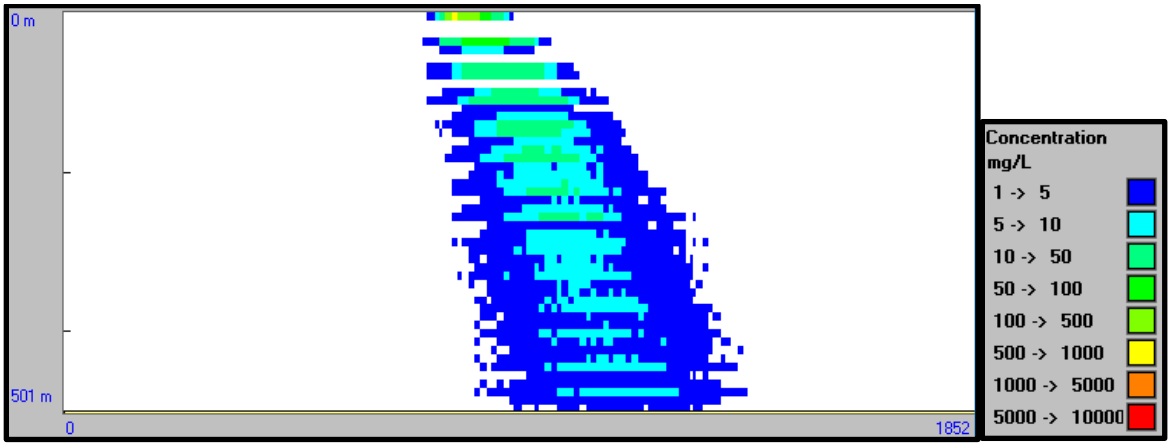


**Figure 4-28. Cross sectional view of predicted water column concentration from an accidental surface release of 60 m$^3$ at Site 2 release site (Winter).**

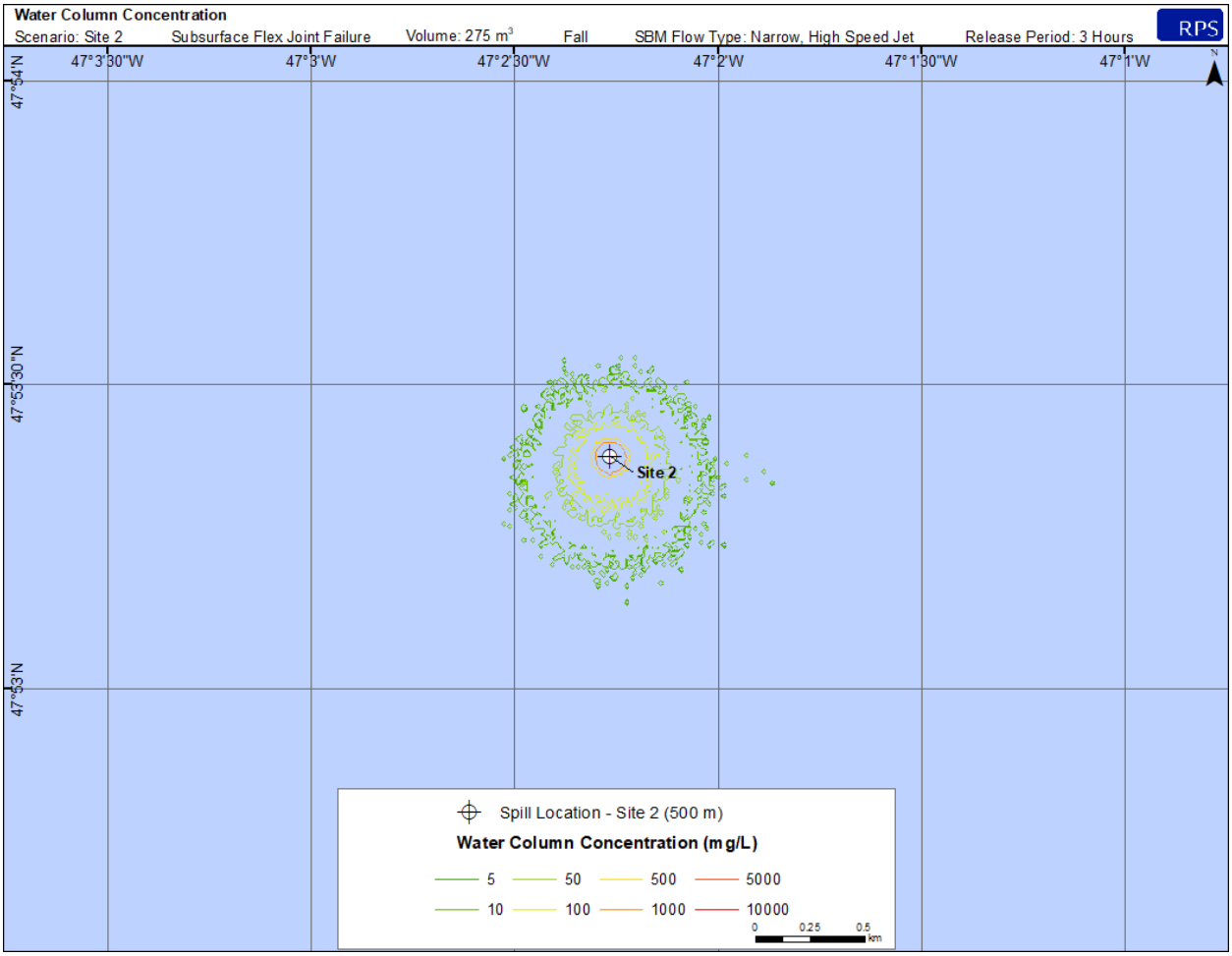


**Figure 4-29. Predicted water column concentration from a flex joint failure accidental seabed release 275 m$^3$ at Site 2 release site (Fall).**

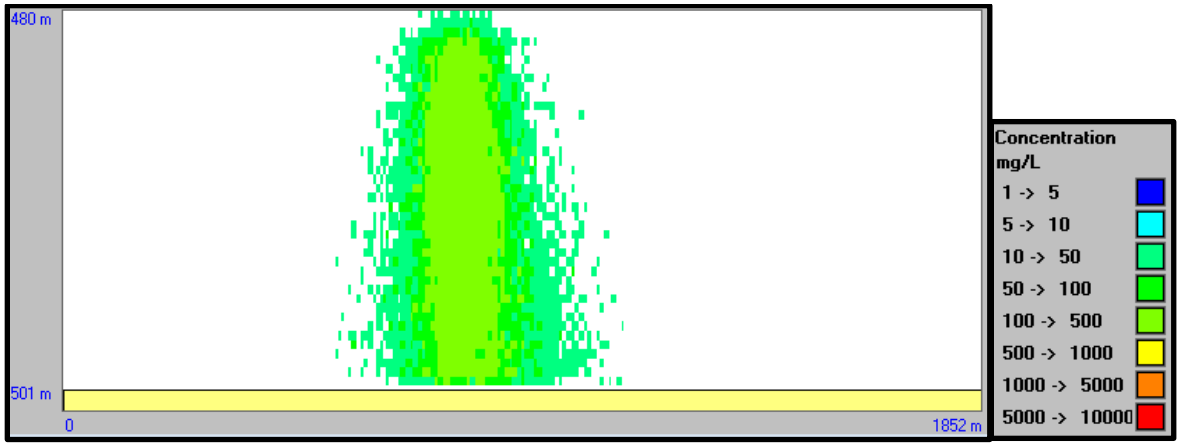


**Figure 4-30. Cross sectional view of predicted water column concentration from a flex joint failure accidental seabed release 275 m$^3$ at Site 2 release site (Fall).**

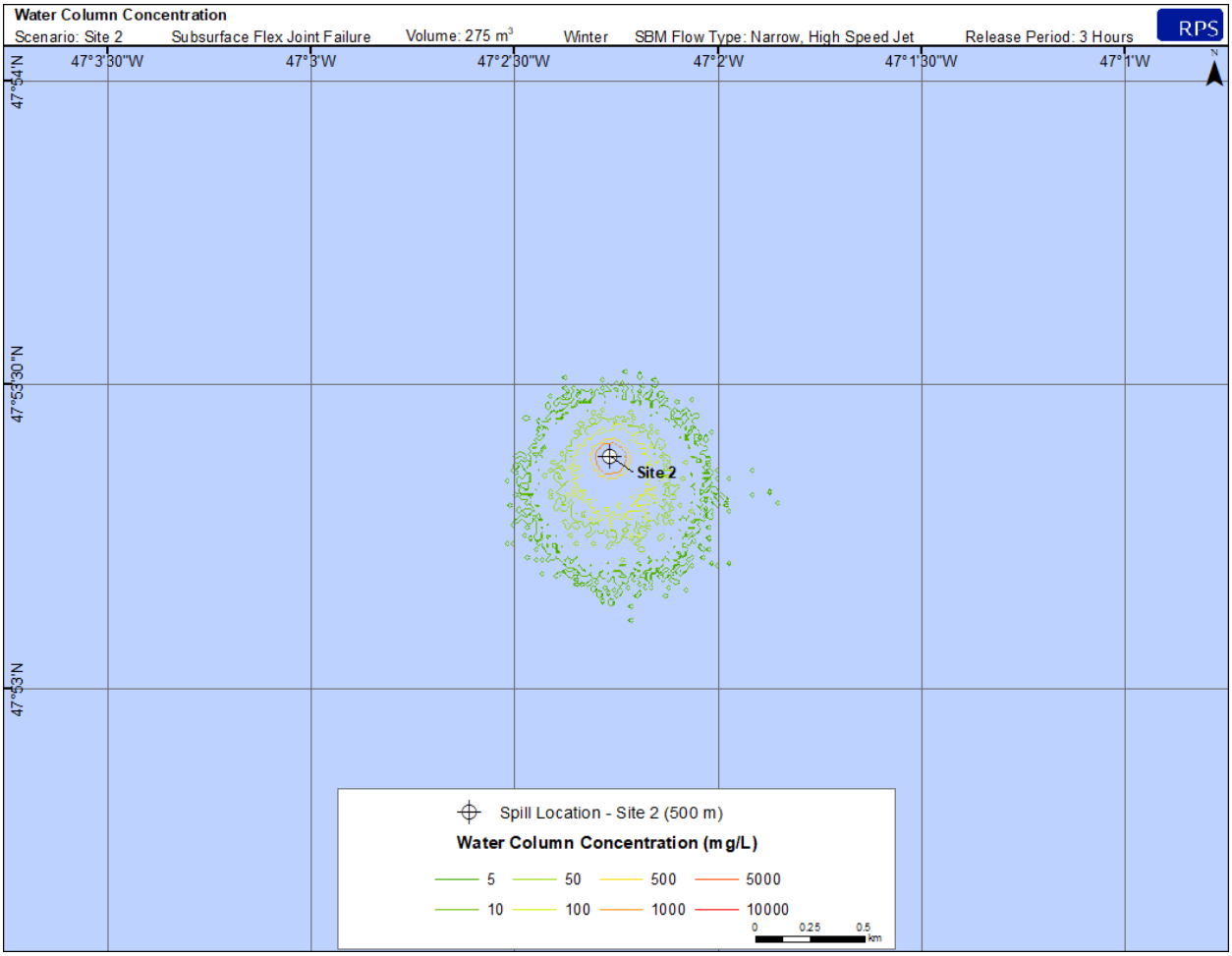


**Figure 4-31. Predicted water column concentration from a flex joint failure accidental seabed release 275 m$^3$ at Site 2 release site (Winter).**

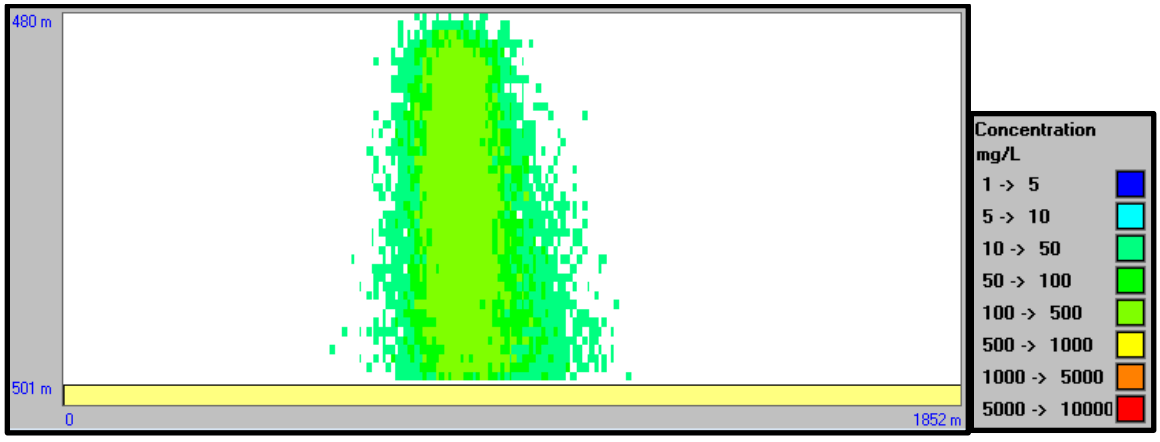


**Figure 4-32. Cross Sectional View of predicted water column concentration from a flex joint failure accidental seabed release 275 m$^3$ at Site 2 release site (Winter).**

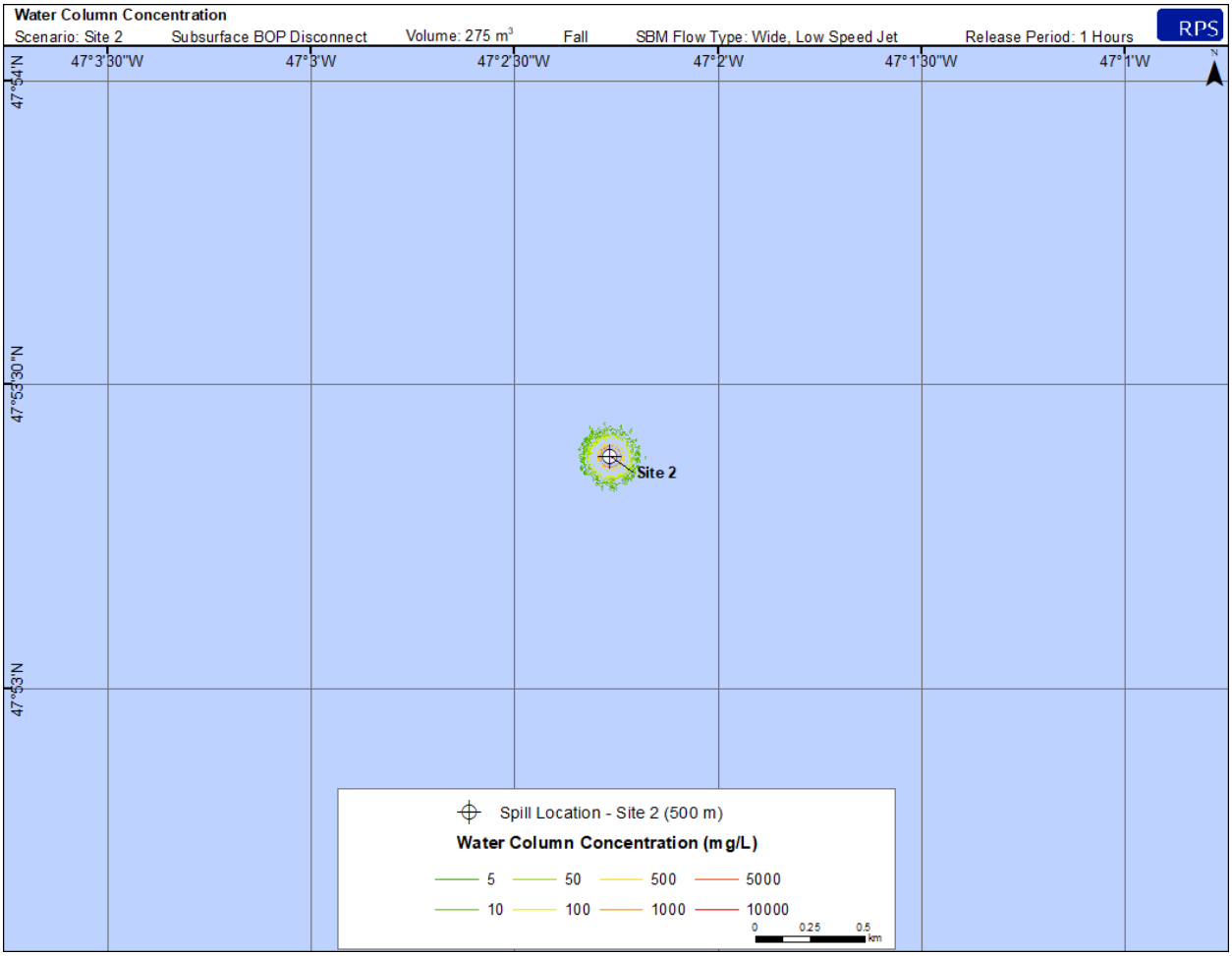


**Figure 4-33. Predicted water column concentration from a BOP disconnect accidental seabed release 275 m$^3$ at Site 2 release site (Fall).**

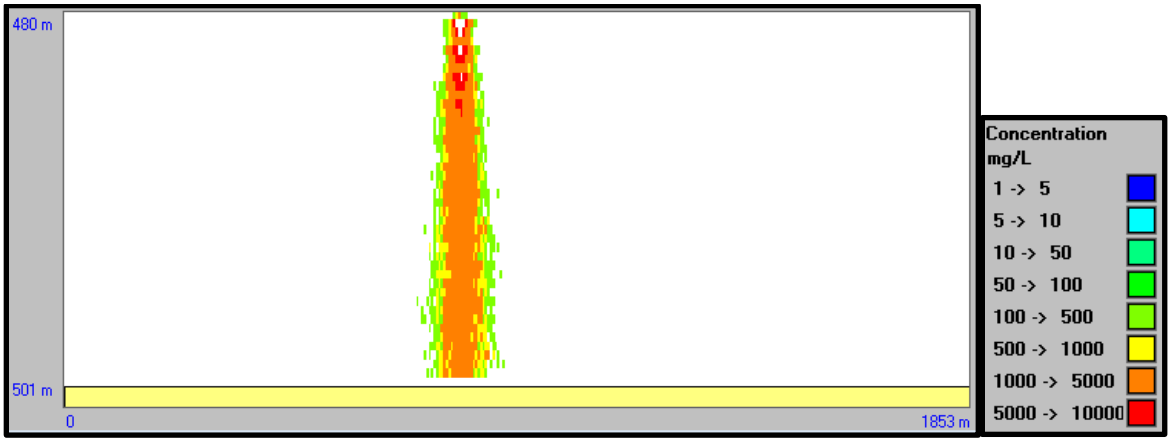


**Figure 4-34. Cross sectional view of predicted water column concentration from a BOP disconnect accidental seabed release 275 m$^3$ at Site 2 release site (Fall).**

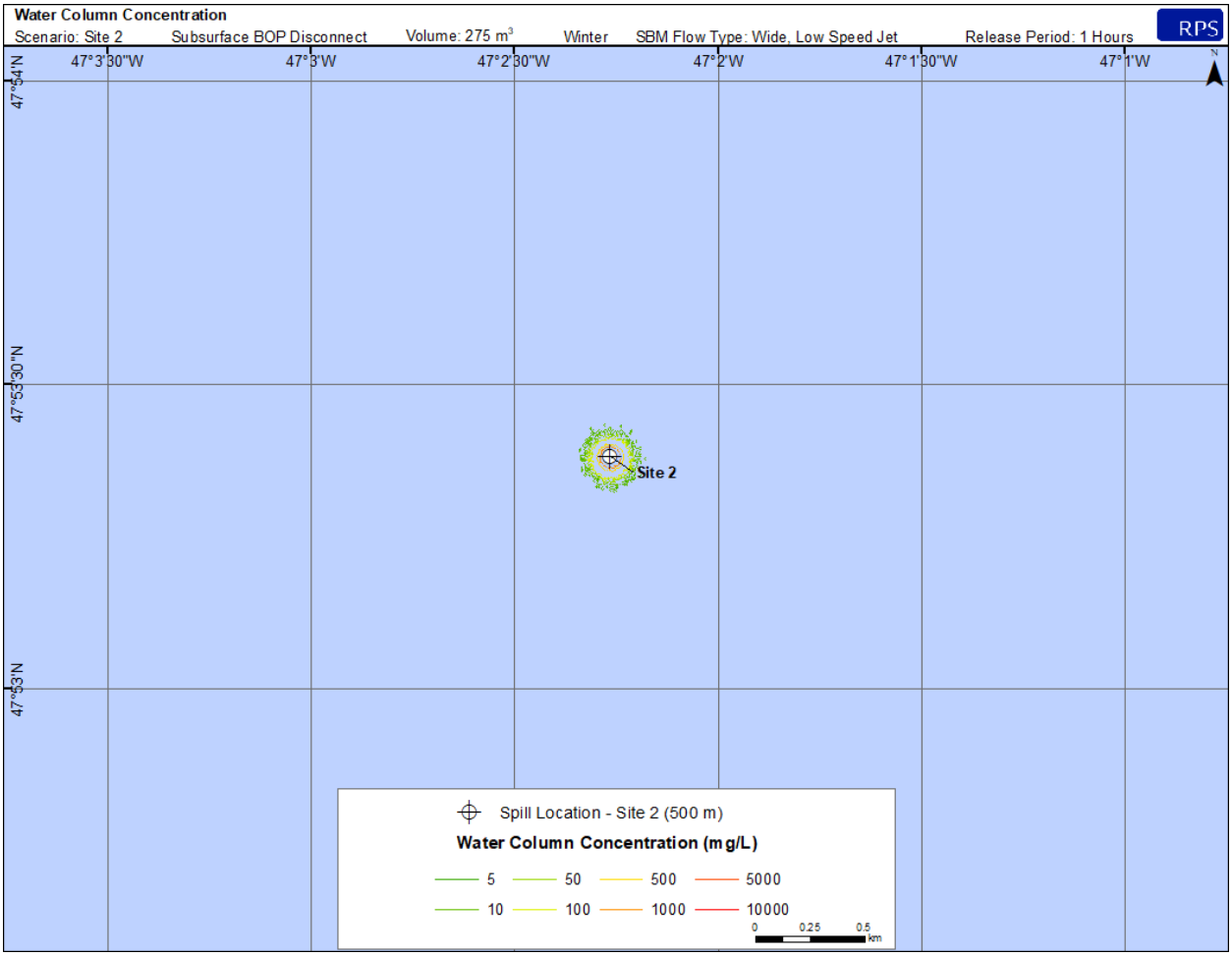


**Figure 4-35. Predicted water column concentration from a BOP disconnect accidental seabed release 275 m$^3$ at Site 2 release site (Winter).**

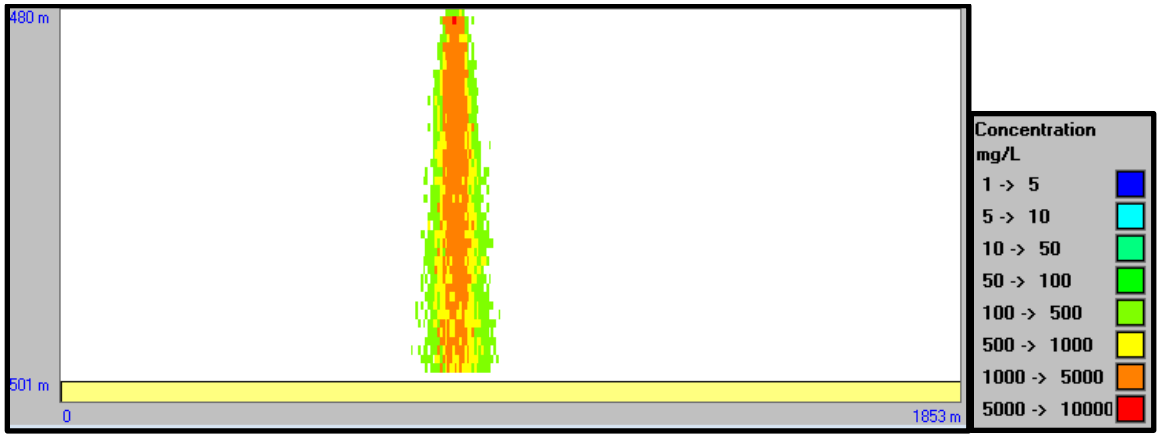


**Figure 4-36. Cross sectional view of predicted water column concentration from a BOP disconnect accidental seabed release 275 m$^3$ at Site 2 release site (Winter).**

### 4.2.3 Summary of Predicted Water Column Concentrations

**Table 4-5. Areal extent of water column concentration (by concentration interval) for Site 1 (Site 1) simulations**

| Water Column Concentration (mg/L) | Cumulative Area Exceeding ($km^2$) | | | | | |
|---|---|---|---|---|---|---|
| | Surface Tank Spill (Fall) | Surface Tank Spill (Winter) | Flex Joint Failure (Fall) | Flex Joint Failure (Winter) | Subsea BOP Disconnect (Fall) | Subsea BOP Disconnect (Winter) |
| 5 | 0.0623 | 0.1059 | 0.23984 | 0.2465 | 0.02121 | 0.02126 |
| **10** | **0.02704** | **0.04861** | **0.23984** | **0.2465** | **0.02121** | **0.02126** |
| 50 | 0.00377 | 0.00347 | 0.23984 | 0.2465 | 0.01431 | 0.0145 |
| **100** | **0.00103** | **0.0013** | **0.08369** | **0.08862** | **0.01197** | **0.01194** |
| 500 | 0 | 0 | 0.01087 | 0.01097 | 0.00511 | 0.00515 |
| **1,000** | **0** | **0** | **0.00677** | **0.0071** | **0.00321** | **0.00304** |
| 5,000 | 0 | 0 | 0.00093 | 0.00101 | 0.00041 | 0.00042 |
| **10,000** | **0** | **0** | **0.00019** | **0.00025** | **0.00004** | **0.00004** |

**Table 4-6. Areal extent of water column concentration (by concentration interval) for Site 2 (Site 2) simulations**

| Water Column Concentration (mg/L) | Cumulative Area Exceeding ($km^2$) | | | | | |
|---|---|---|---|---|---|---|
| | Surface Tank Spill (Fall) | Surface Tank Spill (Winter) | Flex Joint Failure (Fall) | Flex Joint Failure (Winter) | Subsea BOP Disconnect (Fall) | Subsea BOP Disconnect (Winter) |
| 5 | 0.06277 | 0.10505 | 0.24469 | 0.25215 | 0.02114 | 0.0213 |
| **10** | **0.03508** | **0.05157** | **0.24469** | **0.25215** | **0.02114** | **0.0213** |
| 50 | 0.0088 | 0.01073 | 0.08584 | 0.0902 | 0.01449 | 0.01458 |
| **100** | **0.00341** | **0.00455** | **0.04306** | **0.04656** | **0.01191** | **0.01192** |
| 500 | 0.00014 | 0.00015 | 0.01087 | 0.01102 | 0.00501 | 0.00503 |
| **1,000** | **0** | **0** | **0.00662** | **0.00686** | **0.00322** | **0.00321** |
| 5,000 | 0 | 0 | 0.00101 | 0.00109 | 0.0004 | 0.00037 |
| **10,000** | **0** | **0** | **0.00022** | **0.00015** | **0.00004** | **0.00006** |

**Table 4-7. Maximum distance of water column concentration contours (distance from release site) for Site 1 (Site 1) simulations.**

| Deposition Thickness (mm) | Maximum extent from release site (km) | | | | | |
|---|---|---|---|---|---|---|
| | Surface Tank Spill (Fall) | Surface Tank Spill (Winter) | Flex Joint Failure (Fall) | Flex Joint Failure (Winter) | Subsea BOP Disconnect (Fall) | Subsea BOP Disconnect (Winter) |
| 10 | 0.2 | 0.4 | 0.48 | 0.56 | 0.11 | 0.11 |
| 100 | 0.03 | 0.03 | 0.27 | 0.32 | 0.07 | 0.08 |
| 1,000 | 0 | 0 | 0.05 | 0.06 | 0.04 | 0.04 |
| 10,000 | 0 | 0 | 0.01 | 0.01 | 0 | 0 |

**Table 4-8. Maximum distance of water column concentration contours (distance from release site) for Site 2 (Site 2) simulations.**

| Deposition Thickness (mm) | Maximum extent from release site (km) | | | | | |
|---|---|---|---|---|---|---|
| | Surface Tank Spill (Fall) | Surface Tank Spill (Winter) | Flex Joint Failure (Fall) | Flex Joint Failure (Winter) | Subsea BOP Disconnect (Fall) | Subsea BOP Disconnect (Winter) |
| 10 | 0.13 | 0.3 | 0.51 | 0.52 | 0.11 | 0.11 |
| 100 | 0.06 | 0.08 | 0.19 | 0.27 | 0.07 | 0.08 |
| 1,000 | 0 | 0 | 0.06 | 0.06 | 0.04 | 0.04 |
| 10,000 | 0 | 0 | 0.01 | 0.01 | 0.01 | 0.01 |

## 4.3 Model Results Summary

Seabed Deposition

At both sites, deposition resulted in predicted sedimentation thicknesses of 49.3 mm for subsurface releases occurring from BOP disconnect (wide orifice, low velocity release 20 m above seafloor), which roughly corresponds to thresholds representing 50% mortality of some benthic species within the deposition area (37 – 79 mm threshold range; Smit et al. 2008). Subsurface releases occurring from flex joint failure (narrow orifice, high velocity release 20 m above seafloor) was predicted to result in 13.7 mm deposition thickness at both sites, a burial depth which epibenthic, filter-feeding species would not likely survive (10 mm threshold; Smit et al. 2008). Near-surface releases occurring from mud tank release (wide, low velocity releases 5 m below surface) were predicted to be limited to thicknesses of 0.263 mm for Site 1 (1,134 m depth) and 0.588 mm for Site 2 (500 m depth), which would be unlikely to negatively affect benthic organisms. Seasonal differences in the areal extent of seabed deposition were

minimal; however, the maximum distance and orientation of the contours was influenced by season. All winter simulations were predicted to result in thicknesses extending farthest from the spill site, typically to the south and southwest. This pattern is most apparent in the surface releases, most notably at Site 1, with the fall simulation resulting in predicted seabed deposition of 0.1 mm extending 810 m from the spill site, compared to 1,460 m in the winter. Minor differences are also observed when comparing thickness contours by different site, season, and release scenario. As expected, the largest difference are observed when comparing surface releases to subsea releases. Thicknesses > 0.1 mm are observed up to 0.19647 $km^2$ for surface releases from Site 1 during the Fall, down to 0.03525 $km^2$ for subsea BOP releases from Site 2 during the Winter. However subsea BOP releases result in the largest area exceeding 20 mm, up to 0.00428 $km^2$, while other release simulations (surface, or flex joint failure) do not result in thicknesses this high.

Water Column Concentrations

Subsurface releases occurring from flex joint failure (narrow orifice, high velocity release 20 m above seafloor) result in TSS concentrations > 10,000 mg/L surrounding the spill location (within 10 m). These simulations result in maximum concentrations up to 14,700 mg/L. Subsurface releases occurring from BOP disconnect (narrow orifice, high velocity release) also result in 10,000 mg/L concentration contours at both sites with maximum concentrations up to 16,856 mg/L. These relatively high maximum concentrations of TSS are likely to reduce the light available for phytoplankton productivity briefly before the suspended particulates settle out but are not likely to represent toxicity towards water column organisms (IOGP, 2016). Surface releases occurring from mud tank release (wide orifice, low velocity releases) were predicted to be limited to concentrations of 178 mg/L for Site 1 and 696 mg/L for Site 2. Seasonal differences in water column concentration were minimal in the predicted areal extent (except for surface releases); however, the maximum distance and orientation of the contours was predicted to be influenced by seasonal variation. Most winter simulations were predicted to result in the plume extending furthest from the spill site, typically to the south, southwest. This pattern was exaggerated in the surface releases, especially at Site 2, with the fall simulation resulting in water column concentrations of 100 mg/L extending up to 60 m from the spill site, compared to 80 m in the winter. Minor differences are also observed when comparing the areal extents of concentration contours by different site, season, and release scenario. TSS concentrations are observed localized to the release site and cover up to 0.00025 $km^2$ for subsea flex joint releases from Site 1 during the winter, while surface releases do not exceed concentrations this high.

# 5 Discussion and Conclusions

At both drilling locations, measurable thicknesses (0.1 mm) were predicted from accidental releases of SBM in the project area were expected to be contained within 1.5 km of the spill location. Surface releases of SBM were predicted to result in seabed deposition extending farthest from the spill location, due to intensified currents at the surface and longer time over which the sediments settle. Site depth has the potential to increase the extent of predicted deposition but also generally reduces the total deposit thicknesses within the broader area. In the simulations presented above, the extent of deposition from surface releases was predicted to be greater during winter conditions due to enhanced transport by prevailing currents. Subsurface releases occurring from a BOP disconnect near the seafloor were expected to result in the largest overall thicknesses of deposition due to the faster settling time of particles released from a wide orifice, low velocity flow incident, which reduced overall lateral transport.

The variations within predicted results between simulations were due to three main factors including: 1) release height relative to the seabed, 2) settling velocity associated with low versus high velocity releases, and 3) current patterns. Releases resulting from accidental mud tank spillage and BOP disconnect occur at a lower flow rate, and therefore would have faster settling times and thicker deposition within an area that is close to the spill site. Specifically, areal extent affected by surface releases are the most different across site due to difference in depth. Flex joint failure releases typically resulted in increased flow rate, making particles much smaller and therefore decreasing settling rates, which allowed for particles to travel further before being deposited on the seafloor.

The releases modelled in this study may be considered representative of other potential releases in the project area. The depth of the Site 1 and Site 2 sites (1,134 and 500 m, respectively) are similar in depth to other sites within the Project Area.

The hypothetical accidental releases modelled in this study are not intended to predict a specific future event, but rather are to be used as a tool in environmental assessments and spill contingency planning. The results presented in this document demonstrate that there are a range of potential trajectories that could result if a release of synthetic based drilling mud were to occur. The specific trajectories vary for each release based upon the nature of the release, the environmental conditions, and the properties of the fluids. While each accidental release is unique and therefore uncertainties exist, the results of this modelling study suggest that if SBM were to be released in the project Area, there is the potential for measurable seabed deposition to extend 1.5 km from the spill site. In addition, there is the potential for water column concentrations to exceed 10,000 mg/L within 10 m of the spill locations.

# 6 References

Bakhtyar, S., and M.M. Gagnon. 2012. Toxicity assessment of individual ingredients of synthetic-based drilling muds (SBMs). Environ. Monitor. Assess. 184:531105325.

Bleck, R., 1998: Ocean modeling in isopycnic coordinates. Chapter 18 in Ocean Modeling and Parameterization, E. P. Chassignet and J. Verron, Eds., NATO Science Series C: Mathematical and Physical Sciences, Vol. 516, Kluwer Academic Publishers, 4223-448.

Bleck, R. 2002. An oceanic general circulation model framed in hybrid isopycnic-cartesian coordinates. Ocean Modeling, 4, 55-88.

Brandsma, M.G. and J.P. Smith. (1999). Offshore Operators Committee mud and produced water discharge model – report and user guide. Exxon Production Research Company, December 1999.

Burns, K.A., Codi, S., Swannell, R.J.P. & Duke, N.C. (1999) Assessing the degradation potential of endogenous micro-organisms in tropical wetlands. Mangroves and Salt Marshes, 2, 63–74.

Canada-Newfoundland and Labrador Offshore Petroleum Board (C-NLOPB). 2014. Eastern Newfoundland Strategic Environmental Assessment. Final Report. Prepared by AMEC Environment & Infrastructure, AMEC TF 1382502. Available: http://www.cnlopb.ca/pdfs/enlsea/ch1-3.pdf?lbisphpreq=1. Accessed: March 2017.

Chassignet, E. P., L. T. Smith, R. Bleck, and F. O. Bryan. 1996. A model comparison: numerical simulations of the North and Equatorial Atlantic oceanic circulation in depth and isopycnic coordinates. J. Phys. Oceanogr., 26, 1849-1867.

Chandrasekara, W.U., and C.L.J. Frid. 1998. A laboratory assessment of the survival and vertical movement of two epibenthic gastropod species, Hydrobia ulvae and Littorina littorea, after burial in sediment. Journal of Experimental Marine Biology and Ecology 221(2): 191-207.

Cooper, M. and K.A. Haines, 1996.Altimetric assimilation with water property conservation. Journal of Geophysical Research, vol. 24, pp. 1059-1077.

Cummings, J.A. 2005. Operational multivariate ocean data assimilation. Quarterly Journal of the Royal Meteorological Society. Part C, 133(613), 3583-3604.

Ellis, J.I., G. Fraser, and J. Russell. 2012. Discharged drilling waste from oil and gas platforms and its effects on benthic communities. Marine Ecology Progress Series. Vol. 456: 285-302.

Gates A.R. and D.O.B. Jones. 2012. Recovery of benthic megafauna from anthropogenic disturbance at a hydrocarbon drilling well (380 m depth in the Norwegian Sea). PLoS ONE, 7, e44114.

Francingues, N. R., and Palermo, M. R. 2005. “Silt curtains as a dredging project management practice,” DOER Technical Notes Collection (ERDC TN-DOER-E21). U.S. Army Engineer Research and Development Center, Vicksburg, MS.

Gage, John D., and Paul A. Tyler. 1991 Deep-sea biology: a natural history of organisms at the deep-sea floor. Cambridge University Press, 504 pp.

Gates A.R. and D.O.B. Jones. 2012. Recovery of benthic megafauna from anthropogenic disturbance at a hydrocarbon drilling well (380 m depth in the Norwegian Sea). PLoS ONE, 7, e44114.

General Bathymetric Chart of the Oceans (GEBCO). 2003. Centenary Edition of the GEBCO Digital Atlas, published on behalf of the Intergovernmental Oceanographic Commission (IOC) and the International Hydrographic Organization (IHO) as part of the General Bathymetric Chart of the Oceans; British Oceanographic Data Centre (BODC), Liverpool.

Gibbs, R.J., M.D. Matthews, and D.A. Link. 1971. The relationship between sphere size and settling velocity. Journal of Sedimentary Research, v. 41, 7-18.

Glover, A. G. and C. R. Smith. 2003. The deep-sea floor ecosystem: current status and prospects of 706 anthropogenic change by the year 2025. Environmental Conservation 30, 219-241.

Halliwell, G. R., Jr., 1997.Simulation of decadal/interdecadal variability the North Atlantic driven by the anomalous wind field. Proceedings, Seventh Conference on Climate Variations, Long Beach, CA, 97-102.

Halliwell, G. R., Jr., 1998. Simulation of North Atlantic decadal/multi-decadal winter SST anomalies driven by basin-scale atmospheric circulation anomalies. Journal of Physical Oceanography, 28, 5-21.

Halliwell, G.R. 2002.HYCOM Overview. http://www.hycom.org. June 27, 2011.

Halliwell, G. R., Jr., R. Bleck, and E. Chassignet, 1998. Atlantic Ocean simulations performed using a new hybrid-coordinate ocean model. EOS, Fall 1998 AGU Meeting.

Halliwell, G .R, R. Bleck, E. P. Chassignet, and L.T. Smith, 2000: mixed layer model validation in Atlantic Ocean simulations using the Hybrid Coordinate Ocean Model (HYCOM). EOS, 80, OS304.

Han, G. and C.L. Tang, 1999. Velocity and transport of the Labrador Current determined from altimetric, hydrographic, and wind data. Journal of Geophysical Research: Oceans Banner. Volume 4, Issue C8, 15 August 1999. pp. 18047-18057.

Hernández Arana, H.A., R.M. Warwick, M.J. Attrill, A.A. Rowden, and G. Gold-Bouchot. (2005). Assessing the impact of oil-related activities on benthic macroinfauna assemblages of the Campeche shelf, southern Gulf of Mexico. Marine Ecology Progress Series. Vol. 289:89-107.

Hu, D., 1996: On the Sensitivity of Thermocline Depth and Meridional Heat Transport to Vertical Diffusivity in OGCMs. J. Physical Oceanography, 26, 1480-1494.

Hutchison, Z.L., V.J. Hendrick, M.T. Burrows, B. Wilson, and K.S. Last. 2016. Buried alive: the behavioural response of the mussels, Modiolus modiolus and Mytilus edulis to sudden burial by sediment. PLoS ONE 11(3): e0151471. doi: 10.1371/journal.pone.0151471.

International Association of Oil & Gas Producers (IOGP). 2016. Environmental fates and effects of ocean discharge of drill cuttings and associated drilling fluids from offshore oil and gas operations. Report 543. Version 1.0 March 2016. First release. 144 pp.

King, B., and F.A. McAllister, 1997. Modeling the dispersion of produced water discharge in Australia, Volume I and II. Australian Institute of Marine Science report to the APPEA and ERDC.

King, B., and F.A. McAllister, 1998. Modeling the dispersion of produced water discharges. APPEA Journal 1998, pp. 681-691.

Kjeilen-Eilertsen, G., H. Trannum, R. Jak, M. Smit, J. Neff, and G. Durell. (2004). Literature report on burial: derivation of PNEC as component in the MEMW model tool. ERMS Report no. 9B. Report AM 2004/024. 25 pp.

Marsh, R., M. J. Roberts, R. A. Wood, and A. L. New, 1996: An intercomparison of a Bryan-Cox-type ocean model and an isopycnic ocean model, part II: the subtropical gyre and meridional heat transport. J. Phys. Oceanogr., 26, 1528-1551.

Nedwed, T.J & Smith, J & Brandsma, M.G. 2004. Verification of the OOC Mud and Produced Water Discharge Model using lab-scale plume behaviour experiments. Environmental Modelling & Software. 19. 655-670. 10.1016/j.envsoft.2003.08.004.

New, A. and R. Bleck, 1995: An isopycnic model of the North Atlantic, Part II: interdecadal variability of the subtropical gyre. J. Phys. Oceanogr., 25, 2700-2714.

New, A., R. Bleck, Y. Jia, R. Marsh, M. Huddleston, and S. Barnard, 1995: An isopycnic model of the North Atlantic, Part I: model experiments. J. Phys. Oceanogr., 25, 2667-2699.

Paine, M. D., E. M. DeBlois, B. M. Kilgour, E. Tracy, P. Pocklington, R. D. Crowley, U. P. Williams, G. G. Janes. 2014. Effects of the Terra Nova offshore oil development on benthic macro-invertebrates over 10 years of development drilling on the Grand Banks of Newfoundland, Canada. Deep Sea Res. II 110, 38–64.

Petrie, B., 1983. Circulation of the Newfoundland Continental Shelf. Atmosphere-Ocean, vol. 21, no. 2, pp. 207-226.

Petrie, B. A. Isenor, 1985. The Near-Surface Circulation and Exchange in the Newfoundland Grand Banks Region. Atmosphere-Ocean, vol. 23, no. 3, pp. 209-227.

Richardson, P.L., 1983. Eddy Kinetic Energy in the North Atlantic From Surface Drifters. Journal of Geophysical Research, vol. 88, no. C7, pp. 4355-4367.

Roberts, M. J., R. Marsh, A. L. New, and R. A. Wood, 1996: An intercomparison of a Bryan-Cox-type ocean model and an isopycnic ocean model, part I: the subpolar gyre and high latitude processes. J. Phys. Oceanogr., 26, 1495-1527.

Smit, M.G.D., Tamis, J.E., Jak, R.G, Karman, C.C., Kjeilen-Eilertsen, H., Trannum, H. and J. Neff. 2006. Threshold levels and risk functions for non-toxic sediment stressors: burial, grain size changes and hypoxia. Summary. ERMS Report no. 9.

Smit, M.G., K. I. Holthaus, H. C. Trannum, J. M. Neff, G. Kjeilen-Eilertsen, R. G. Jak, I. Singsaas, M. A. Huijbregts, A. J. Hendriks. 2008. Species sensitivity distributions for suspended clays, sediment burial, and grain size change in the marine environment. Environmental Toxicology and Chemistry. 27(4):1006-12.

Southwest Research Institute. 2003. Drill cuttings fall velocity tests. Final Report submitted to the American Petroleum Institute. San Antonio, Texas. SwRI Project 18.06134.

Southwest Research Institute. 2007. Fall Velocity of Synthetic-Based Drilling Fluids in Seawater. Final Report Prepared for Minerals Management Service. San Antonio, Texas. SwRI Project 18.12210.

Statoil 2016. Response to Comments – 2016 Drilling EA Amendment. SC-CNO-0122-16. December 15, 2016.

Spaulding, M. L., T. Isaji, and E. Howlett. 1994. MUDMAP: A model to predict the transport and dispersion of drill muds and production water, Applied Science Associates, Inc, Narragansett, RI.

Trannum, H. C., A. Setvik, K. Norling, H. C. Nilsson. 2011. Rapid macrofaunal colonization of water-based drill cuttings on different sediments. Marine Pollution Bulletin 62, 2145-2156.

United States Coast Guard (USCG). 2009. How do the Labrador and Gulf Stream Currents Affect Icebergs. Labrador and Gulf Stream currents affect icebergs in the North Atlantic Ocean. USCG Navigation Center. U.S. Department of Homeland Security. Available: https://navcen.uscg.gov/?pageName=iipHowDoTheLabradorAndGulfStreamCurrentsAffectIcebergsInTheNorthAtlanticOcean. Accessed: March 2017.

Volkov, D.L., 2005. Interannual Variability of the Altimetry-Derived Eddy Field and Surface Circulation in the Extratropical North Atlantic Ocean in 1993-2001. Journal of Physical Oceanography, Vol. 35, pp. 405-426.

Wilber, D. H., W. Brostoff, D. G. Clarke, G. L. Ray. 2005. Sedimentation: potential biological effects of dredging operations in estuarine and marine environments. US Army Engineer Research and Development Center DOER-E20pg. 15 pp.

Wood Group PLC. 2018. Drill Cuttings Dispersion Modeling Bay du Nord Development Project. Prepared for Equinor Canada Ltd., St. John's, Prepared by Wood Environmental & Infrastructure Solutions, St. John's, October 2018.